https://doi.org/10.5194/egusphere-2026-4247
Preprint. Discussion started: 22 July 2026

Future scenarios of thunderstorm environments in Fennoscandia based on a regional climate model

Meri Virman[1], Terhi K. Laurila[1], Antti Mäkelä[1], Petter Lind[2], Anna Luomaranta[1], and Hilppa Gregow[1]
[1]Finnish Meteorological Institute, Helsinki, Finland
[2]Rossby Centre, Swedish Meteorological and Hydrological Institute, Norrköping, Sweden
Correspondence: Meri Virman (meri.virman@fmi.fi)

Abstract.
This study investigates how increasing greenhouse gas concentrations may affect environmental conditions favourable for thunderstorms over Fennoscandia. The future scenarios are based on data produced with the HARMONIE-Climate convection-permitting regional climate model forced by two global climate models at the lateral boundaries. The distribution of thunderstorm-favourable days, defined as days with co-occurring conditional instability and precipitation, in model data compares well with observed thunder days in May–September 2002–2018 across the study domain. By 2081–2100, the area-average frequency of favourable days is projected to increase by approximately 40–185 % in Finland, 30–185 % in Sweden, and 15–210 % in Norway relative to 1986–2005 under the RCP4.5 and RCP8.5 emission scenarios. Projected increases are largest over the northern Fennoscandia and in simulations exhibiting stronger warming. Thunderstorm-favourable conditions occurring simultaneously with strong vertical wind shear are also simulated to become more common, suggesting more frequent potential for severe organized convection in a future climate. More research is needed to understand how the changes in general storm-favourable environmental conditions may affect actual hazard occurrence. The results support the use of the HARMONIE-Climate model for convective storm scenario studies and offer valuable context for climate change adaptation in Fennoscandia.

1 Introduction

Thunderstorms can cause a wide range of impacts, including infrastructure damage, lightning-induced wildfires, crop losses caused by hail, as well as fallen trees and power outages from downbursts, destructive straight-line winds and tornadoes. Society and sectors such as forestry and emergency services and insurance companies benefit from increased understanding of how the occurrence of thunderstorms might change in a warming climate. This enables better risk assessment, supports long-term adaptation planning, and improves preparedness.

In Fennoscandia (specifically Finland, Sweden and Norway), the majority of thunderstorms occur during a relatively short time period between May–September (Mäkelä et al., 2014). Despite the northern location and less frequent conditions suitable for the formation of thunderstorms than elsewhere in Continental Europe (Enno et al., 2020; Taszarek et al., 2020a), the Fennoscandian countries experience frequent lightning (Mäkelä et al., 2014), severe-wind-producing mesoscale convective systems (MCSs) and derechos (Punkka et al., 2006; Punkka and Bister, 2015; Toll et al., 2015; Rantala et al., 2026), large hail

https://doi.org/10.5194/egusphere-2026-4247
Preprint. Discussion started: 22 July 2026

(Tuovinen et al., 2009, 2015), heavy rain (Dyrrdal et al., 2021; Utriainen et al., 2025), and, on occasion, tornadoes (Rauhala et al., 2012; Antonescu et al., 2016).

Assessing the observed long-term occurrence of convective storms and trends in the past is difficult due to the limited temporal and spatial coverage of observations, which can result in storm impacts being missed (e.g. Groenemeijer et al., 2017; Allen, 2018; Taszarek et al., 2019). Furthermore, weather and climate models often struggle to simulate the initiation and evolution of convective storms because they involve processes occurring at sub-grid scales (Allen, 2018). Consequently, both past and future changes in convective storms have often been assessed indirectly from reanalysis and climate model data using storm-favourable environmental conditions as proxies for convective hazards (e.g. Brooks et al., 2003; Brooks, 2013; Trapp et al., 2007, 2009; Diffenbaugh et al., 2013; Groenemeijer et al., 2017; Púčik et al., 2017; Allen, 2018; Taszarek et al., 2021a, b).

The ingredients required for the development of deep moist convection and (severe) thunderstorms are the presence of conditional instability, a moist lower-troposphere, and a trigger mechanism forcing vertical lifting of air parcels (Doswell et al., 1996). Even though lightning is the result of complex cloud-scale interactions, the probability for a thunderstorm can be estimated to some degree from the occurrence of conditional instability (Taszarek et al., 2017; Ukkonen et al., 2017), since lightning occurrence is strongly linked to convectively available potential energy (CAPE, Westermayer et al., 2017). Strong vertical wind shear, together with strong CAPE, has been shown to be a good indicator for the occurrence of severe thunderstorms (Brooks et al., 2003; Púčik et al., 2015; Punkka and Bister, 2015; Taszarek et al., 2017). This is because strong shear favors the organization of deep convection and can lead to significant hail-producing supercells or long-lasting MCSs capable of producing widespread damage and lightning (Weisman and Klemp, 1982). However, even if convective instability and strong shear are present, the occurrence of (severe) convection is not guaranteed. Inhibiting factors, such as a dry low-to-mid troposphere or the presence of convective inhibition (CIN), can suppress the growth of convective updrafts or inhibit thunderstorm formation altogether (Westermayer et al., 2017). Furthermore, severe convection can occur in the absence of strong shear (e.g. local downbursts) and the formation of a specific surface hazard requires more complex conditions, such as large low-level lapse rate in environments conducive to strong surface wind gusts (Taszarek et al., 2017).

Despite these limitations, several studies have used combinations of parameters such as convective instability, vertical wind shear, precipitation and CIN as proxies to isolate thunderstorm-favourable conditions (e.g. Brooks et al., 2003; Brooks, 2013; Trapp et al., 2007, 2009; Diffenbaugh et al., 2013; Groenemeijer et al., 2017; Púčik et al., 2017; Allen, 2018; Taszarek et al., 2021a, b). For example, Taszarek et al. (2021a) and Púčik et al. (2017) quantified thunderstorm and severe thunderstorm environments in ERA5 reanalysis data and the EURO-CORDEX regional climate model data, respectively, based on the co-occurrence of convective instability, deep layer vertical wind shear (DLS) and precipitation exceeding specific thresholds. Although these proxies cannot be used to reproduce the actual numbers of observed storms, they capture the main ingredients of (severe) thunderstorms and can be used to assess changes in the situations that increase the likelihood for storm development (Allen, 2018; Taszarek et al., 2019, 2021a, b).

Other studies focusing on specific hazards, such as lightning, strong wind gusts and large hail, have made use of statistical or machine learning models to calculate observed hazard probabilities from environmental conditions (Rädler et al., 2018, 2019; Torralba et al., 2023; Cui et al., 2026; Battaglioli et al., 2026), or utilized (additional) process-based diagnostics from high-

https://doi.org/10.5194/egusphere-2026-4247
Preprint. Discussion started: 22 July 2026

resolution climate models. Examples for the latter include the use of model simulated vertical velocity and cloud microphysical properties in studies of the occurrence of lightning and hail (Brisson et al., 2021; Kahraman et al., 2025; Cui et al., 2025) and modeled wind gusts to estimate changes in convective winds (Brown et al., 2024).

Increases in lower-tropospheric temperature have been shown to lead to more frequent conditionally unstable situations through increased near-surface moisture (Púčik et al., 2017; Rädler et al., 2018, 2019; Taszarek et al., 2021a). This is expected to increase the frequency of conditions conducive to (severe) thunderstorms as the climate warms in large parts of Europe, including Fennoscandia (Púčik et al., 2017; Rädler et al., 2018, 2019). However, it remains unclear whether these changes lead to increased hazard occurrence due to potential counteracting changes in convective initiation (see e.g. Taszarek et al., 2021a) and storm-scale controls on hazard formation (Kahraman et al., 2025), and studies have pointed out contradicting results using different methodologies (Brisson et al., 2021; Kahraman et al., 2025).

Only a few European studies on the future scenarios of thunderstorms include analysis of the Fennoscandian region (Púčik et al., 2017; Wennerdahl, 2017; Rädler et al., 2019). Furthermore, it remains unclear to what extent the EURO-CORDEX models used in the studies by Púčik et al. (2017) and Rädler et al. (2019), which apply deep convection parameterization schemes, can adequately represent the processes relevant for thunderstorm development and the Fennoscandian climate. Recently, a climate scenario dataset was produced for Fennoscandia using the regional climate model HARMONIE-Climate (HCLIM), applied at a convection-permitting horizontal grid resolution (Lind et al., 2023). Generally, convection-permitting climate models with km-scale spatial resolution have been shown to lead to more realistic convective initiation, storm organization and precipitation distribution than models with coarser resolution and parameterized convection (e.g. Lucas-Picher et al., 2021).

In this study, we use HCLIM data to explore the possible future changes in the frequency of days with conditions favourable for (severe) thunderstorm development under different greenhouse gas concentration scenarios in Fennoscandia. While the use of a convection-permitting climate model such as HCLIM could enable a more process-based approach to diagnose the occurrence of lightning or other hazards, we instead apply simple threshold-based proxies used in previous studies to provide a general understanding of potential changes in the key ingredients that favour thunderstorm development. We first compare the proxy variables simulated by HCLIM with reanalysis data and observations to provide context regarding the capability of the HCLIM model and proxy to represent the environments and observed thunderstorm climate. We then present the projected changes for different regions of Fennoscandia.

This study is organized as follows. Section 2 provides an overview of the model, observational and reanalysis datasets used, followed by a description of the proxies and metrics applied. Section 3 presents the results of the comparative analysis between model, observations and reanalyses, while Section 4 examines the projected changes in storm-favourable environments. The results are discussed in Section 5 and summarized in Section 6.

https://doi.org/10.5194/egusphere-2026-4247
Preprint. Discussion started: 22 July 2026

2 Data and methods

2.1 HARMONIE-Climate simulations

The HCLIM regional climate model is the climate version of the HIRLAM-ALADIN Research on Mesoscale Operational NWP in Euromed (HARMONIE) system (Bengtsson et al., 2017) and is developed and maintained in a consortium consisting of members from multiple national institutes in Europe (Lindstedt et al., 2015; Belušić et al., 2020). Here, we use output from convection-permitting simulations with HCLIM cycle 38, applied at 3 km horizontal grid resolution over Fennoscandia. The multi-decadal climate simulations have been produced in a Nordic collaboration as part of the Nordic Convection Permitting Climate Projections (NorCP) project (Lind et al., 2020, 2023).

The convection-permitting configuration of HCLIM has been extensively evaluated against observations in Fennoscandia by Lind et al. (2020), Médus et al. (2022), and An et al. (2026), and shown to be in good agreement with regional high-resolution observations in terms of warm-season precipitation and temperature distributions. It also provides significant added value for the representation of summertime convective precipitation and precipitation over complex topography compared to models with a coarser resolution (Lind et al., 2020, 2023; Médus et al., 2022; Utriainen et al., 2025; Xie et al., 2025).

The HCLIM simulations have been made by utilizing a double nested approach. First, the global ERA-Interim reanalysis (Dee et al., 2011) or a global climate model (GCM) provided initial and lateral boundary conditions for the HCLIM-ALADIN configuration at 12 km spatial resolution nested over an extended domain that covers a large part of Europe and the eastern North Atlantic. The 12 km simulation provides lateral boundary conditions for the convection-permitting HCLIM-AROME configuration at 3 km spatial resolution every 3 hours. HCLIM-ALADIN and HCLIM-AROME used a time step of 300 and 75 seconds respectively, with 65 levels in the vertical. From stored output, we obtained surface precipitation rate at 1-hourly time resolution and northward and eastward near-surface and 500 hPa-level wind speed and CAPE at 3-hourly time resolution.

HCLIM-AROME treats deep convection explicitly, allowing a more realistic representation of many deep convective circulations. However, important processes influencing the formation and evolution of convection, such as microphysical and boundary layer processes, remain parameterized. For example, the condensation and evaporation of hydrometeors, which indirectly affect the organisation of deep convection through the formation of downdrafts and cold pools, are represented using a single-moment bulk microphysics scheme. A detailed description of HCLIM cycle 38 can be found in Belušić et al. (2020).

The HCLIM dataset comprises multi-decadal simulations made with different lateral boundary conditions and greenhouse gas scenarios (Table 1). A hindcast simulation (HCLIM-ERAI), obtained by downscaling ERA-Interim for 1998–2018, provides a model-based reconstruction of past climate for evaluation against observations. Future projections follow the Representative Concentration Pathways (RCPs, Moss et al., 2010; Van Vuuren et al., 2011) scenarios with a radiative forcing of 4.5 W m^{-2} (RCP4.5) or 8.5 W m^{-2} (RCP8.5) at the end of the 21st the century. RCP8.5 simulations are driven by two GCMs from the CMIP5 ensemble (EC-Earth v3 and GFDL-CM3, Hazeleger et al., 2012; Donner et al., 2011), whereas only EC-Earth is used for RCP4.5. These are referred to as HCLIM-ECE and HCLIM-GFDL, respectively, or collectively as HCLIM-GCM. The HCLIM-GCM simulations cover 1986–2005 (historical, "hi"), 2041–2060 (mid-century, "mc"), and 2081–2100 (late-century, "lc").

https://doi.org/10.5194/egusphere-2026-4247
Preprint. Discussion started: 22 July 2026

Both HCLIM-ECE and HCLIM-GFDL exhibit biases from the forcing GCM and/or HCLIM (Lind et al., 2023). For projected climate change, EC-Earth (HCLIM-ECE) is close to the CMIP5 ensemble mean in terms of the increase in 2m temperature over northern Europe by the end of the 21st century, whereas GFDL-CM3 (and HCLIM-GFDL) represents a model with a stronger rise in temperature and more rapid changes in the Nordic region (Lind et al., 2023).

Table 1. Overview of the HCLIM simulations.

Simulation name	Time period	Lateral boundary conditions	Scenario
HCLIM-ERAI	1998–2018	ERA-Interim	–
HCLIM-ECE-hi	1986–2005	EC-Earth	–
HCLIM-ECE-RCP4.5-mc	2041–2060	EC-Earth	RCP4.5
HCLIM-ECE-RCP4.5-lc	2081–2100	EC-Earth	RCP4.5
HCLIM-ECE-RCP8.5-mc	2041–2060	EC-Earth	RCP8.5
HCLIM-ECE-RCP8.5-lc	2081–2100	EC-Earth	RCP8.5
HCLIM-GFDL-hi	1986–2005	GFDL	–
HCLIM-GFDL-RCP8.5-mc	2041–2060	GFDL	RCP8.5
HCLIM-GFDL-RCP8.5-lc	2081–2100	GFDL	RCP8.5

2.2 NORDLIS lightning observations

The Nordic Lightning Information System (NORDLIS) is a cooperative, ground-based lightning location network operated jointly by the national meteorological institutes of the Nordic and Baltic countries. The network currently covers Finland, Sweden, Norway, Estonia, Latvia, and Lithuania, providing real-time and archived lightning observations across northern Europe. Full operational coverage has been available since 2002, making NORDLIS one of the longest continuously operating regional lightning detection networks at high latitudes (Mäkelä et al., 2014).

A thunder day (thunderstorm day or keraunic level) is the oldest meteorological variable regarding thunderstorms giving information of the local occurrence of thunderstorms. While a thunder day does not indicate the intensity of the thunderstorm, it is a usable parameter for showing the overall local daily occurrence of deep-moist convection. Although a thunder day is originally determined by human observers (WMO, 1956), it can also be derived from lightning location data as described by Mäkelä et al. (2014). The method uses the spatio-temporal information of lightning data and examines those grid points that are within the audible radius (about 10 km) from the located lightning. A thunder day is counted if at least one lightning is within the audible radius. In this study, thunder days are analysed from the lightning location data from the period 2002–2018, and the final outputs have been regridded to the HCLIM 3 km grid.

https://doi.org/10.5194/egusphere-2026-4247
Preprint. Discussion started: 22 July 2026

2.3 ERA5

The ERA5 reanalysis (Hersbach et al., 2020) has been developed by the European Centre for Medium Range Weather Forecasting (ECMWF). It combines a data assimilation system and the numerical weather prediction model Integrated Forecasting System (IFS) cycle Cy41r2 to provide a "best" estimate of the state of the atmosphere. The underlying IFS model contains parameterization schemes for several subgrid-scale atmospheric process (Hersbach et al., 2020), including a mass-flux parameterization scheme for deep convection (Bechtold et al., 2014). ERA5 data is obtained from the Climate Data Store, which provides data at a horizontal resolution of 0.25 degrees (roughly 31 km), a temporal resolution of 1 hour and a vertical resolution of 137 model levels from 1940 to present day. In this study, the obtained ERA5 variables are CAPE, total and convective precipitation, and 10-m and 500-hPa u and v-wind components.

2.4 Proxies for thunderstorm environments

We define simple physically motivated proxies for (severe) thunderstorm environments adapted from previous pan-European studies (Taszarek et al., 2019, 2020b, 2021a, b; Púčik et al., 2017). Specifically, a "thunderstorm environment" is defined as a day with at least one simultaneous occurrence of instantaneous CAPE exceeding 150 J kg^{-1} and a subsequent 3-hourly precipitation amount exceeding 0.5 mm. Second, a "severe thunderstorm environment" is defined analogously but includes an additional requirement that DLS, computed from the same timestep as CAPE, exceeds 12.5 m s^{-1}. A day with at least one 3-hourly timestep with instantaneous CAPE $>$ 150 J kg^{-1}, DLS $>$ 12.5 m s^{-1} or 3-hourly precipitation $>$ 0.5 mm are referred to as a "CAPE environment", "DLS environment" and "precipitating environment", respectively.

The proxies represent the main ingredients for (severe) thunderstorm development. The presence of CAPE indicates potential for deep convection and lightning, while the DLS threshold restricts the environments to those supportive of organized severe convection (Westermayer et al., 2017; Taszarek et al., 2017; Ukkonen et al., 2017). As a proxy for convective initiation, we require the presence of at least some precipitation to increase the likelihood that (precipitating) convection forms (Trapp et al., 2009; Púčik et al., 2017; Taszarek et al., 2019, 2021a, b).

HCLIM CAPE is based on the most unstable parcel between the surface and approximately 350 hPa level, found using mixed-layer parcels near the surface and single-level parcels aloft. DLS is defined as the bulk vertical wind shear between the near-surface wind vector and the wind vector at the 500 hPa level. Although DLS is traditionally computed over the 0–6 km layer, we do not interpolate to the 6 km level due to the relatively coarse vertical resolution of the HCLIM output data, as in Púčik et al. (2017) and Rädler et al. (2019).

To facilitate a brief comparison of the proxy variables between HCLIM and ERA5 reanalysis data, similar thresholds are also applied to ERA5 data. CAPE from ERA5 is the maximum CAPE produced by air parcels departing at model levels below the 350 hPa level. Although the vertical resolution of ERA5 supports the calculation of 0–6 km shear, DLS is calculated similarly as that from HCLIM to support comparison.

The CAPE threshold (150 J kg^{-1}) is close to the minimum CAPE observed prior to non-severe and severe thunderstorms in Finland (Ukkonen et al., 2017; Punkka and Bister, 2015) and is consistent with the criterion for mixed-layer CAPE used in

https://doi.org/10.5194/egusphere-2026-4247
Preprint. Discussion started: 22 July 2026

previous pan-European studies utilizing ERA5 reanalysis data (Taszarek et al., 2020b, 2021a, b, note that mixed-layer CAPE was not available from HCLIM). The selected DLS threshold (12.5 m s^{-1}) is close to the median 0–6 km shear (10 m s^{-1}) observed in environments of severe wind-producing MCSs in Finland (Punkka and Bister, 2015), and aligns with the 0–6 km shear criterion used for derecho-favourable environments in Finland by Rantala et al. (2026). Lastly, defining the threshold for precipitation amount is challenging since convection can be associated with any amount of precipitation. The threshold of at least 0.5 mm $(3h)^{-1}$ of precipitation is close to the thresholds used for convective or total precipitation (ranging from 0.25 mm h^{-1} to 1 mm $(6h)^{-1}$) in previous studies using other datasets (Taszarek et al., 2021a; Púčik et al., 2017).

Taszarek et al. (2021a) incorporated a composite severity parameter combining instability and DLS, defined as $\sqrt{2 \times CAPE} \times DLS$, as an additional criterion in their severe thunderstorm environments proxy. The composite parameter (CAPESHEAR) has been shown to effectively discriminate between non-severe and severe thunderstorms (e.g. Taszarek et al., 2017). We do not include the CAPESHEAR parameter in our primary proxy, but instead briefly analyse its changes separately as a complementary metric of convective severity since similar parameters are widely used in early-warning systems (Tsonevsky et al., 2018). Following Taszarek et al. (2021a), we define a CAPESHEAR environment as a day with at least one occurrence of CAPESHEAR > 500 m^2 s^{-2}.

2.5 Metrics calculated from HCLIM data

The criteria for the proxy parameters are applied to HCLIM data at every 3 km × 3 km grid box and 3-hourly timestep. Then, the days with at least one proxy occurrence within a grid box or a given subregion are identified. The daily aggregation provides a metric that is easily interpretable and can be qualitatively compared with observed thunder days.

The seasonal (May–September) mean number of environments and thunder days are quantified on a point-by-point basis to obtain an estimate for how often a given location (3 × 3 km area) experiences favourable environments. However, the likelihood for a storm (environment) in a given grid box is quite small, and changes calculated per grid box may be affected by different storm trajectories in different model time periods. Therefore, changes from the baseline period to the future periods are investigated also by computing the relative change in the area average number of proxy occurrences in six regions with different thunderstorm climatologies, that span the southern and northern parts of the Fennoscandian countries (see regions in Fig. 2a in Sect. 3.2).

Changes in area-average local frequency do not directly imply changing number of storm-favourable days overall in the region, and may instead reflect more widespread favourable conditions. It is therefore useful to spatially aggregate the environments (and observed thunder days) and investigate how often a region experiences at least one storm environment somewhere, and how this might change. The number of days with at least one proxy occurrence anywhere within the six regions between May–September are computed and referred to as a regional occurrence. However, we note that the number of grid boxes differs between the regions, and should be compared with caution.

https://doi.org/10.5194/egusphere-2026-4247
Preprint. Discussion started: 22 July 2026

3 Comparative analysis of thunderstorm environments in historical HCLIM data, reanalysis and observations

The individual proxy components from the HCLIM-ERAI hindcast simulation are first compared with ERA5 to provide context regarding the performance of HCLIM in representing the statistics of convective storm ingredients (Sect. 3.1). However, a perfect agreement cannot be expected, as ERA5 also contain biases, employs a parameterized deep convection scheme, and has a coarser spatial resolution than HCLIM (Taszarek et al., 2021c). Nevertheless, it can be still considered as the best available reference data.

Then, the long-term occurrence and spatial distribution of (severe) thunderstorm environments in HCLIM-ERAI are compared with observed thunder days to gain understanding of whether the proxy (and HCLIM) are physically reasonable and can represent the observed thunder day climatology (Sect. 3.2). However, the model-based estimates use precipitation as a proxy for storm initiation and therefore cannot be expected to reproduce actual observed numbers due to simplified assumptions. Thus, perfect correspondence is neither expected nor physically meaningful.

Lastly, regional models using GCMs as lateral boundaries typically inherit biases from the parent models. Thus, we also examine the capability of the historical HCLIM-ECE and HCLIM-GFDL simulations to replicate the distributions from HCLIM-ERAI and observations where applicable (Sect. 3.3).

3.1 Individual proxy components in HCLIM-ERAI hindcast simulation and ERA5

The spatial distributions of CAPE (> 150 J kg^{-1}), precipitating (> 0.5 mm (3h)$^{-1}$) and DLS (> 12.5 m s^{-1}) environments are broadly similar in HCLIM-ERAI and ERA5 (in 1998–2018, Fig. 1). In both datasets, CAPE environments occur most frequently in the southern parts of the Fennoscandian countries and over the Baltics (Fig. 1a-b). Both datasets show a distinct local minimum in the occurrence of CAPE environments over the Scandinavian mountain range. We note that differences between HCLIM and ERA5 may partly arise from different calculation methodologies of CAPE, although both are calculated using the most unstable parcel. Regardless, the absolute numbers of CAPE environments from HCLIM compares well with that from ERA5 (Fig. 1a–b).

In terms of precipitating environments, HCLIM-ERAI and ERA5 also show a similar spatial pattern. A distinct maximum in the frequency of precipitating environments extends along the western coast of Norway (Fig. 1c–d), likely produced by frequent extratropical cyclone activity and orographic enhancement of precipitation with westerly winds. ERA5 shows a systematically higher number of precipitating environments than HCLIM-ERAI (Fig. 1c-d) across the entire domain. However, rather than suggesting a systematic bias in HCLIM-ERAI, the frequency of precipitating environments in ERA5 is likely overestimated due to the relatively coarse horizontal resolution of ERA5 (approximately 31 km) and associated overestimation of weak precipitation. Lastly, both datasets show that the occurrence of DLS environments is the highest along the coast of Norway, in southern Sweden and near the eastern border of the study domain, and the lowest over and around the Scandinavian mountain range (Fig. 1e–f). While of similar magnitude, DLS environments are somewhat more frequent in HCLIM-ERAI than in ERA5.

https://doi.org/10.5194/egusphere-2026-4247
Preprint. Discussion started: 22 July 2026

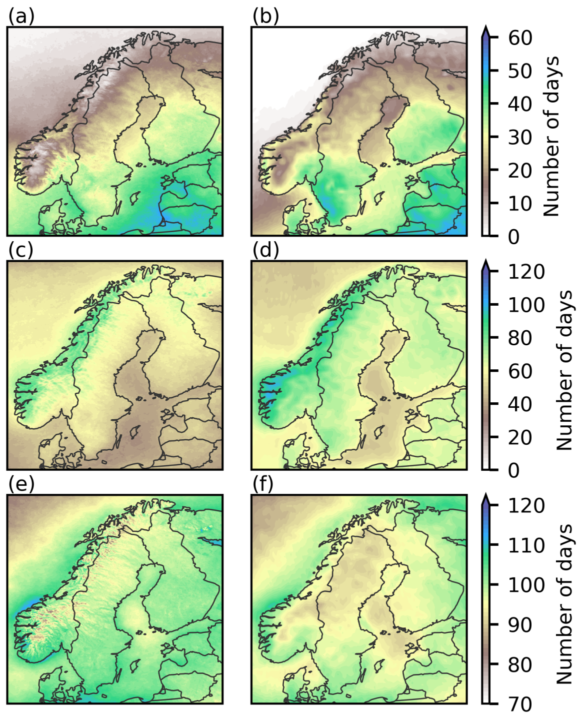

Figure 1. Seasonal (May–September) mean number of days with at least one occurrence of (a)–(b) CAPE > 150 J kg^{-1}, (c)–(d) precipitation > 0.5 mm (3h)$^{-1}$ and (e)–(f) DLS > 12.5 m s^{-1} in HCLIM-ERAI (left column) and ERA5 (right column) in 1998–2018. Both datasets are in their native grid. Note that (d) presents total precipitation from ERA5.

3.2 Storm environments in HCLIM-ERAI hindcast simulation and observations

Figure 2a shows the seasonal mean number of observed thunder days derived from the NORDLIS lightning network in 2002–2018. The three Fennoscandian countries exhibit a clear north-south gradient in observed thunder days, with the most frequent occurrence in the southern half of the countries. However, in Norway, the distribution is more complex, with large spatial variability, and a distinct minimum along the Scandinavian mountain range. In all countries, some regions experience over 15 local (within 3 km $\times$ 3 km area) thunder days per year. The area average numbers over the southern and northern subregions (see regions in Fig. 2a) are presented in Table 2.

Applying the proxy for thunderstorm environment to HCLIM-ERAI data in 2002–2018 yields a monthly (not shown) and spatial distribution of seasonal (Fig. 2b) mean number of thunderstorm-favourable days that resembles the observed pattern of thunder days (Fig. 2a). The spatial pattern of severe thunderstorm environments (Fig. 2c) in HCLIM also resembles that of the observed thunder days (Fig. 2a) and simulated thunderstorm-favourable days (Fig. 2b), although the frequency is substantially lower. The spatial distribution of storm environments (Fig. 2b–c), and observed thunder days (Fig. 2a), appears to be generally

https://doi.org/10.5194/egusphere-2026-4247
Preprint. Discussion started: 22 July 2026

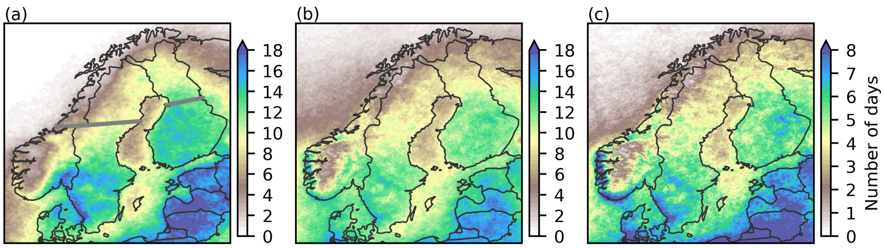

Figure 2. Seasonal (May–September) mean number of (a) observed thunder days from NORDLIS, and days that meet the criteria for (b) thunderstorm environment and (c) severe thunderstorm environment in HCLIM-ERAI in 2002–2018. The border of the southern and northern regions of Finland, Sweden and Norway referred to in the text are marked in grey.

governed by the distribution of CAPE environments (Fig. 1a–b, note that Fig. 1 shows the 1998–2018 period), indicating that the southern Fennoscandia experiences more frequent thunder days mainly due to more frequent unstable conditions.

Despite qualitatively similar spatial patterns, the seasonal mean local number of thunderstorm environments in HCLIM-ERAI is slightly smaller than the observed number of local thunder days (by 0–4 d y^{-1}) in most of Fennoscandia (Fig. 2a–b), leading to systematic underestimation of the area average local numbers by a few days per year in Finland and Sweden (Table 2). In Norway, the local numbers in HCLIM-ERAI are overestimated compared to observations in many regions, especially along the southwestern coast of Norway, which exhibits a more robust local maximum and higher number of thunderstorm environments (Fig. 2b) than what is indicated by observations (Fig. 2a). As a result, the simulated area average numbers are closer to or slightly higher than observations in Norway (Table 2). The differences between proxy occurrence and observations may arise from (1) biases in HCLIM, (2) too high or low thresholds for proxy components, (3) missing ingredients in the proxy definition, (4) identification of precipitating but non-lightning producing systems occurring in unstable conditions as thunderstorm-favourable environments and (5) uncertain lightning detection near the edge of the observation network.

When the thunderstorm and severe thunderstorm proxies are applied to ERA5 (1998–2018, Fig. A1, note that only the convective precipitation component is used following Taszarek et al. 2021a), the distributions are similar to those produced by HCLIM-ERAI, although ERA5 (Fig. A1d and f) overestimates the frequencies compared to HCLIM-ERAI (Fig. A1c and e) and observations (Fig. 2a). The strong local maximum in southwestern Norway is also present in the distribution of severe thunderstorm environments in HCLIM (Fig. 2c) and when the proxies are applied to ERA5 data (Fig. A1d and f). This implies that the maximum in southwestern Norway in HCLIM-ERAI is not solely related to the underlying model data and may reflect a poorer proxy performance there.

3.3 Storm environments in historical HCLIM-GCM simulations

The spatial distribution, range of spatial variability (Fig. 3a, g) and monthly distribution (not shown) of local thunderstorm environments in HCLIM-ECE-hi and HCLIM-GFDL-hi (1986–2005) are in a good agreement with observed thunder days (2002–2018) and the HCLIM-ERAI hindcast simulation (1998–2018 or 2002–2018) across Fennoscandia (Figs. 2a–b, 3a, d

https://doi.org/10.5194/egusphere-2026-4247
Preprint. Discussion started: 22 July 2026

Table 2. Area average local number of days per year (May–September) that meet the different environment criteria in HCLIM-ERAI (2002–2018) and HCLIM-ECE-hi and HCLIM-GFDL-hi (1986–2005) in the northern (left value) and southern (right value) regions of Finland, Sweden and Norway. For thunderstorm environment, also the area mean local number of observed thunder days in 2002–2018 from NORDLIS is marked. See subregions in Figure 2a.

Environment/proxy	NORDLIS	HCLIM-ERAI	HCLIM-ECE-hi	HCLIM-GFDL-hi
Finland				
Thunderstorm	9.4, 13.4	7.6, 11.9	5.6, 8.8	4.5, 9.0
Severe thunderstorm		3.8, 5.8	2.5, 3.8	2.2, 4.2
CAPESHEAR		3.7, 7.0	2.0, 3.6	1.5, 4.3
CAPE		20.0, 33.6	14.8, 25.4	10.9, 24.3
Precipitating		60.0, 51.9	57.7, 51.0	63.4, 55.9
DLS		97.9, 101.1	98.8, 99.8	102.2, 108.0
Sweden				
Thunderstorm	7.2, 12.5	6.7, 10.9	5.1, 9.0	4.4, 9.8
Severe thunderstorm		3.1, 5.2	1.9, 3.7	1.9, 4.6
CAPESHEAR		2.7, 5.3	1.5, 3.1	1.2, 4.4
CAPE		17.3, 30.3	13.5, 25.0	10.7, 26.5
Precipitating		60.9, 54.3	58.9, 52.9	63.3, 58.0
DLS		95.9, 100.6	95.8, 98.5	99.8, 104.9
Norway				
Thunderstorm	3.3, 7.9	4.1, 8.5	3.8, 9.2	3.0, 9.3
Severe thunderstorm		2.1, 4.1	1.6, 3.6	1.3, 4.0
CAPESHEAR		1.5, 3.3	1.2, 2.4	0.7, 2.7
CAPE		10.1, 20.4	9.0, 20.9	6.5, 20.9
Precipitating		70.5, 67.8	70.0, 68.1	73.5, 71.2
DLS		96.0, 99.4	95.4, 95.3	99.4, 101.3

and g). This demonstrates the ability of both HCLIM-GCM combinations in simulating realistic historical storm environments. However, both HCLIM-GCM combinations show systematic differences, which should be kept in mind when assessing changes simulated by the model. Namely, both HCLIM-ECE-hi and HCLIM-GFDL-hi simulate slightly fewer occurrences than HCLIM-ERAI in Fennoscandia in the majority of grid boxes (Fig. 3a, d, g), which leads to even larger underestimation of area average seasonal occurrence compared to observations than was the case for HCLIM-ERAI in Finland and Sweden (Table 2, see also Sect. 3.2). Part of the difference may be explained by different time periods, however, a bulk of it is likely caused by a cold bias inherited from the GCMs used as lateral boundaries (Lind et al., 2023), which is reflected as a slightly underes-

https://doi.org/10.5194/egusphere-2026-4247
Preprint. Discussion started: 22 July 2026

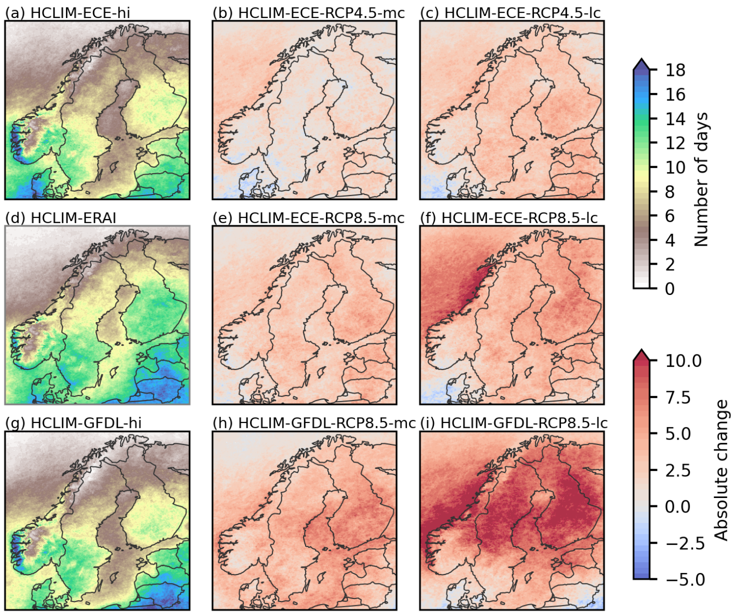

Figure 3. Seasonal (May–September) mean number of days that meet the criteria for thunderstorm environment in (a) HCLIM-ECE-hi in 1986–2005, and its absolute change by mid-century (2041–2060) and late-century (2081–2100) under (b)–(c) HCLIM-ECE-RCP4.5 and (e)–(f) HCLIM-ECE-RCP8.5. Corresponding results for HCLIM-GFDL-hi and HCLIM-GFDL-RCP8.5 are shown in (g)–(i). Panel (d) shows the mean number of days from the HCLIM-ERAI hindcast (1998–2018).

timated number of CAPE environments in many regions in HCLIM-GCM-hi (Table 2). In southern Norway, however, the area average occurrence in HCLIM-GCM-hi is higher than in HCLIM-ERAI and observations (Table 2). This is partly due to highly frequent proxy thunderstorm environments in grid boxes in southwestern Norway in HCLIM-ECE-hi and HCLIM-GFDL-hi (Fig. 3a, d, g), which amplifies the systematic offset found in that region in HCLIM-ERAI compared with observations (Fig. 2a–b, see Sect. 3.2).

In terms of the severe storm proxies, the historical HCLIM-GCM simulations show similar spatial distributions of severe thunderstorm and CAPESHEAR environments than HCLIM-ERAI (Figs. 4 and A2). The occurrence of severe-storm favouring environments is highest in the southernmost regions of Sweden and Norway and in south-to-southeastern Finland across simulations. As was the case for thunderstorm environments, HCLIM-GCM-hi seem to include biases that lead to somewhat underestimated number of severe-storm environments across most regions compared with HCLIM-ERAI (Fig. 4 and A2, Table 2). While the differences in severe environments between HCLIM-ERAI and the HCLIM-GCMs are likely contributed by differences in CAPE, part may be explained also by different number of DLS and precipitating environments (Table 2, see also Figs. 9–11). We note that the mean numbers of CAPESHEAR environments are higher than that of severe thunderstorm environments (Table 2, Fig. A2), likely partly due to the missing criterion for precipitation in the former.

https://doi.org/10.5194/egusphere-2026-4247
Preprint. Discussion started: 22 July 2026

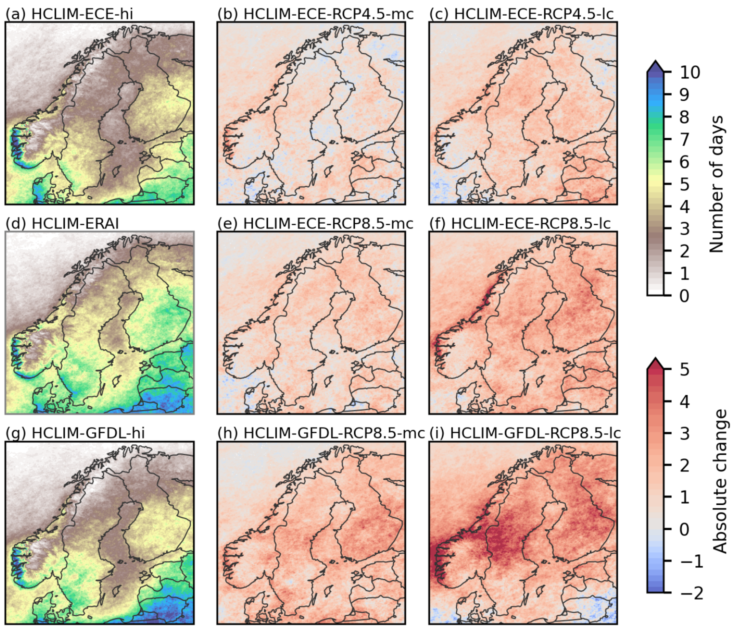

Figure 4. Seasonal (May–September) mean number of days that meet the criteria for severe thunderstorm environment in (a) HCLIM-ECE-hi in 1986–2005, and its absolute change by mid-century (2041–2060) and late-century (2081–2100) under (b)–(c) HCLIM-ECE-RCP4.5 and (e)–(f) HCLIM-ECE-RCP8.5. Corresponding results for HCLIM-GFDL-hi and HCLIM-GFDL-RCP8.5 are shown in (g)–(i). Panel (d) shows the mean number of days from the HCLIM-ERAI hindcast (1998–2018).

3.4 Summary from comparison

Overall, HCLIM-ERAI is in close agreement with ERA5 in the individual proxy components (Fig. 1) and with observed thunder days in the distribution of simulated (severe) thunderstorm environments (Fig. 2, Table 2). The historical HCLIM-GCM simulations show similar spatial patterns to the hindcast simulation and observations, however, the simulated frequencies deviate due to biases that should be kept in mind. Despite the differences between model and observations, the results suggest that HCLIM and the proxies appear suitable for estimating the potential occurrence of thunderstorms, identifying regions with the highest likelihood of thunderstorm occurrence in Fennoscandia, and assessing how favourable conditions may change in the Fennoscandian region in the future. Unlike for thunderstorm environments, no direct observational comparison is possible for severe environments in Fennoscandia due to the lack of long-term, spatially homogeneous data on severe events. Nevertheless, the results suggest that the potential for severe convection is the highest in regions with the most frequent thunderstorm activity.

https://doi.org/10.5194/egusphere-2026-4247
Preprint. Discussion started: 22 July 2026

4 Future scenarios of favourable environments

4.1 Local storm environments

Figure 3 shows that both HCLIM-ECE and HCLIM-GFDL project absolute increases in the seasonal mean number of thunderstorm environments in most of Fennoscandia from the historical period (1986–2005) to mid-century (2041–2060) and late-century (1981–2100) periods. The majority of grid boxes over land in Finland, Sweden and Norway show increased local numbers across simulations (absolute change up to 5 d y^{-1} in HCLIM-ECE-RCP4.5-lc and up to 10 d y^{-1} in HCLIM-GFDL-RCP8.5-lc in a 3 km $\times$ 3 km area), with the exception of HCLIM-ECE-RCP4.5-mc, which shows regions with small decreases. We note, however, that the point-by-point changes are characterized by considerable variability (or noise) that may arise from the stochasticity of thunderstorm environments.

Despite these increases, the spatial pattern of thunderstorm-favourable environments remains largely unchanged from the historical period, with higher local numbers persisting in the southern regions in the future simulations (not shown). An exception is HCLIM-GFDL-RCP8.5-lc, which projects a shift in the maximum occurrence frequency toward central Sweden by the end of the century, however, this feature is not seen in HCLIM-ECE-RCP8.5-lc (not shown).

All subregions of the Fennoscandian countries show projected increases in the area average occurrence of thunderstorm environments (Fig. 5a–c). The increases are generally larger at the end of the century than at mid-century, under RCP8.5 than under RCP4.5, and in HCLIM-GFDL than in HCLIM-ECE. The northern regions of Finland, Sweden and Norway appear to exhibit larger relative increases than the southern regions (Fig. 5a–c; note, however, that the baseline occurrence in the north is smaller than in the south, see Table 2). For the northern regions by the end of the century, HCLIM-ECE projects an increase of about 45–65 % in the area-average occurrence under the RCP4.5 scenario. The projected increases under the high-emission scenario (RCP8.5) are higher, up to about 70–110 % in HCLIM-ECE-RCP8.5-lc and 185–210 % in HCLIM-GFDL-RCP8.5-lc. It should be noted, however, that the baseline area-average number is lower in HCLIM-ECE-GFDL-hi (Table 2), which might partly explain the higher relative increase in HCLIM-ECE-GFDL-RCP8.5 compared with HCLIM-ECE-RCP8.5. In the southern subregions, the level of relative change remains below approximately 40 %, 60 % and 100 % in HCLIM-ECE-RCP4.5-lc, HCLIM-ECE-RCP8.5-lc and HCLIM-GFDL-RCP8.5-lc, respectively. It is also worth noting that, especially in the northern regions, the level of increase according to HCLIM-ECE-RCP8.5 by mid-century is nearly equal to or even exceeding that projected by HCLIM-ECE-RCP4.5 by late-century, highlighting the more rapid and stronger response in the RCP8.5 scenario, likely associated with higher radiative forcing and its impact on thunderstorm-favourable environments.

As for thunderstorm environments, the number of severe thunderstorm environments is projected to increase with higher greenhouse gas concentrations in a point-by-point basis in majority of Fennoscandia (Fig. 4) as well as in terms of the area average occurrences (Fig. 5d–f). The northern parts of Finland, Sweden and Norway exhibit higher relative changes in the area average occurrence than the southern parts of the countries according to almost all simulations (Fig. 5d–f). Specifically, the area average local numbers are projected to increase by about 35–70 % in the north, and by about 15–25 % in the south, by late-century according to HCLIM-ECE-RCP4.5. Again, the changes are more pronounced in RCP8.5 and when GFDL is used

https://doi.org/10.5194/egusphere-2026-4247
Preprint. Discussion started: 22 July 2026

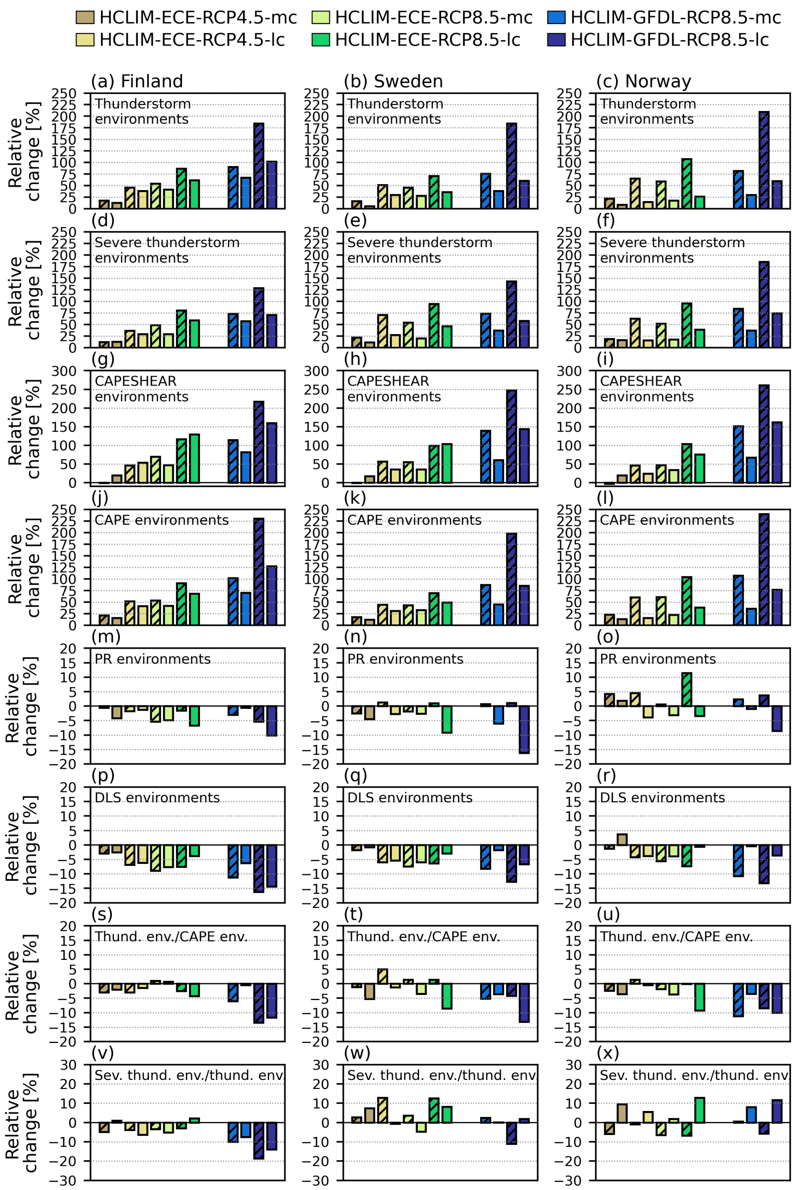

Figure 5. Relative change (%) in the area average number of days per year (May–September) that meet the criteria for (a)–(c) thunderstorm, (d)–(f) severe thunderstorm, and (g)–(i) CAPESHEAR environments, as well as days with at least one occurrence of (j)–(l) CAPE > 150 J kg^{-1}, (m)–(o) 3-hourly precipitation > 0.5 mm, and (p)–(r) DLS > 12.5 m s^{-1}. Also shown are changes in the fraction of (s)–(u) thunderstorm environments from CAPE environments and (v)–(x) severe thunderstorm environments from thunderstorm environments. Results are based on HCLIM-ECE and HCLIM-GFDL simulations for southern (empty bars) and northern (hatched bars) subregions of Finland (left), Sweden (middle), and Norway (right), relative to 1986–2005 for mid-century (2041–2060, mc) and late-century (2081–2100, lc) periods.

https://doi.org/10.5194/egusphere-2026-4247
Preprint. Discussion started: 22 July 2026

as lateral boundary conditions. Namely, the relative increases shown by HCLIM-GFDL-RCP8.5-lc (HCLIM-ECE-RCP8.5) exceed about 125 % (80 %) in the northern regions and are roughly 60–75 % (40–60 %) in the southern regions.

All HCLIM simulations project increases in the occurrence of CAPESHEAR environments (Figs. 5g–j and A2), indicating increased potential for severe convection also using the CAPESHEAR metric. Figure 5g–j shows that, by the late-century, the area average number of CAPESHEAR environments increases between 25–55 % according to HCLIM-ECE-RCP4.5-lc, 75–130 % according to HCLIM-ECE-RCP8.5-lc, and 145–260 % according to HCLIM-GFDL-RCP8.5-lc. Relative increases in the potential for severe convection appear to be higher when quantified using CAPESHEAR than the severe thunderstorm environment proxy under RCP8.5 in late-century. However, differences may arise from the absence of the precipitation requirement in the CAPESHEAR proxy.

4.2 Regional storm environments and monthly distribution

The regional occurrence of thunderstorm-favourable days and observed thunder days in May–September exhibit large interannual variability across regions (Fig. 6). The annual mean regional number of observed thunder days per year is between approximately 63–95 d y^{-1} in Finland, 66–113 d y^{-1} in Sweden and 53–96 d y^{-1} in Norway, with more frequent activity in the southern than in the northern regions (Fig. 6a–b, d–e, g–h). However, HCLIM-ERAI and HCLIM-GCM-hi simulate more frequent thunderstorm environments compared to observed thunder days. This is most distinct in Norway, likely due to the maximum in thunderstorm environments along the western coast of Norway that was less robust in observations (see Sect. 3.2–3.3). The discrepancies should be kept in mind when interpreting the future projections.

The annual mean regional occurrence in northern Finland, Sweden and Norway is projected to increase by around 7–15 d y^{-1} by mid-century, with more pronounced increases by the end of the century (approximately 10–12 d y^{-1} under HCLIM-ECE-RCP4.5-lc and 18–29 d y^{-1} under HCLIM-GCM-RCP8.5-lc, Fig. 6c, f, i). In contrast, in southern Fennoscandia, the increases by mid-century remain below 5 d y^{-1}, except in south Finland in HCLIM-GFDL-RCP8.5-mc that projects an increase of 10 d y^{-1}. With the exception of southern Finland in HCLIM-GFDL-RCP8.5-lc (increase up to 16 d y^{-1}), the increases are generally modest (1–10 d y^{-1}) also by the end of the century.

Conditions favourable for the regional occurrence of severe thunderstorms occur on multiple days per year in all historical HCLIM simulations. Again, the occurrence frequency is higher in the southern regions (Fig. 7). The annual mean occurrence in HCLIM-ERAI and HCLIM-GCM-hi ranges from about 55–78 days in the northern regions to 84–114 days in the southern regions (Fig. 7a–b, d–e, g–h). The annual mean occurrence in the north (south) of Finland, Sweden and Norway is projected to become approximately 5–15 (3–12, Fig. 7c), 5–15 (1–6, Fig. 7f) and 8–25 (3–13, Fig. 7i) d y^{-1}, respectively, higher than in the historical period. The largest increase is projected under RCP8.5 in late-century.

Generally, HCLIM suggests that the southern Fennoscandian regions, where historical regional occurrence of (severe) thunderstorm-favourable days is high (Figs. 6–7), may not experience notable average increases in the frequency of thunderstorm-favourable days overall as the climate warms. However, the large interannual variability in the frequency of (severe) thunderstorm environments, also seen in observed thunder days, is projected to persist as the climate warms in all regions of Fennoscandia, with some years experiencing much more frequent conditions for storm occurrence than others (Fig. 6–7).

https://doi.org/10.5194/egusphere-2026-4247
Preprint. Discussion started: 22 July 2026

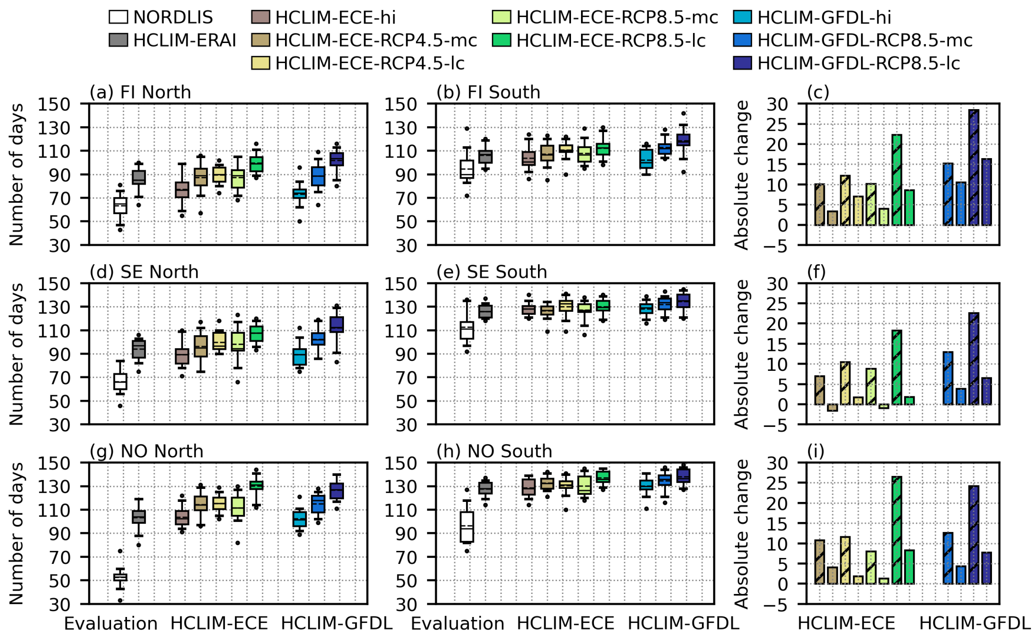

Figure 6. Regional number of days that meet the thunderstorm environment criteria (left, middle), and the change in annual mean with respect to the historical period (right), from HCLIM-ECE and HCLIM-GFDL for two subregions of (a)–(c) Finland, (d)–(f) Sweden and (g)–(i) Norway in September–May. Periods "hi", "mc", and "lc" denote 1986–2005, 2041–2060, and 2081–2100, respectively. Corresponding values from HCLIM-ERAI and the observed regional thunder days from NORDLIS are shown for 2002–2018. Boxplots (left, middle) represent interannual variability, with middle solid (dashed) line representing the mean (median), boxes the 25th and 75th percentiles and whiskers the 1st and 99th percentiles. Southern and northern regions are marked with empty and hatched bars, respectively.

The distribution of monthly mean regional occurrence of thunderstorm environments shows that conditions favourable for thunderstorms occur on average most frequently during June–July–August, which is consistent with observed thunder days (Fig. 8a–b, e–f, i–j). The northern regions exhibit generally fewer thunderstorm environments throughout the season and a more distinct mid-summer peak compared to the southern regions. HCLIM projects absolute increases in the monthly mean occurrence of regional thunderstorm environments in the north throughout the thunderstorm season (Fig. 8c–d, g–h, k–l). However, there is no clear systematic shift in the monthly distribution as the seasonal distribution of increases varies between simulations. For example, HCLIM-ECE-RCP8.5-lc shows larger increases in the beginning and end of the season, whereas HCLIM-GFDL-RCP8.5-lc projects the largest increases generally in August–September. In contrast, the southern regions show a more consistent response across simulations, namely, most HCLIM simulations indicate that increases occur mainly in May and/or September, when the historical frequency of environments is relatively low. During July–August, when the occurrence peaks (also in observations), projected changes are more modest (or even negative).

https://doi.org/10.5194/egusphere-2026-4247
Preprint. Discussion started: 22 July 2026

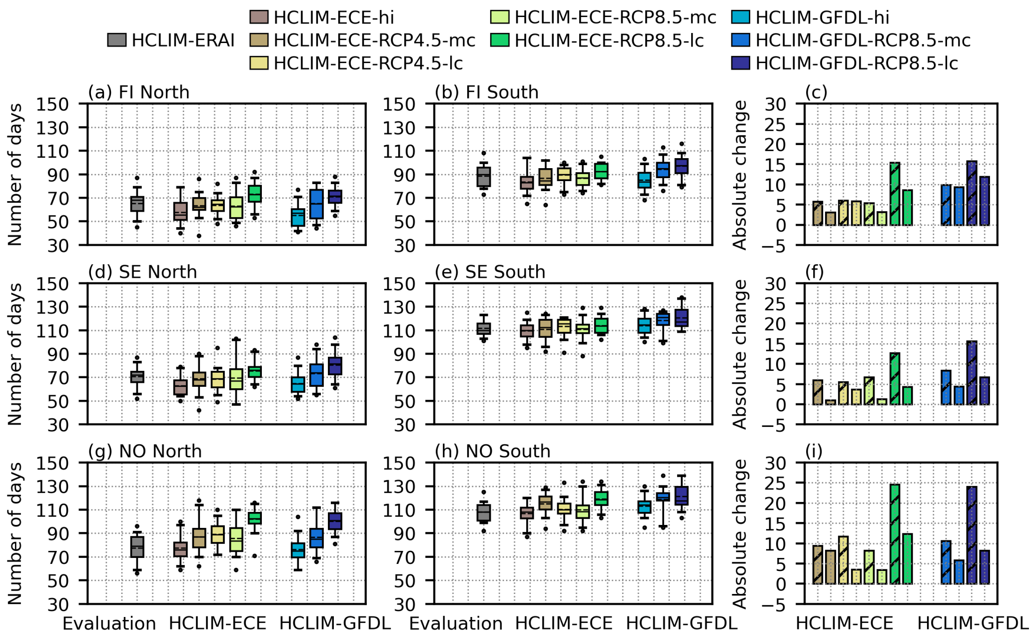

Figure 7. Regional number of days that meet the severe thunderstorm environment criteria (left, middle), and the change in annual mean with respect to the historical period (right), from HCLIM-ECE and HCLIM-GFDL for two regions of (a)–(c) Finland, (d)–(f) Sweden and (g)–(i) Norway in September–May. Periods "hi", "mc", and "lc" denote 1986–2005, 2041–2060, and 2081–2100, respectively. Corresponding values from HCLIM-ERAI are shown for 2002–2018. Boxplots (left, middle) represent interannual variability, with middle solid (dashed) line representing the annual mean (median), boxes the 25th and 75th percentiles and whiskers the 1st and 99th percentiles.

Overall, Figure 8 suggests that thunderstorm-favourable days Fennoscandia are likely to become more common throughout the warm season, particularly at the beginning and end of the warm season, however, changes outside the May–September period are outside of the scope of this study.

4.3 Future scenarios of individual proxy components

The previous sections established projected increases in the occurrence of (severe) thunderstorm environments, and generally larger relative increases in the northern than southern regions. We now examine how the individual proxy components are simulated to change in order to gain insights into the main drivers of change in the storm environments.

Across Fennoscandia, all HCLIM simulations suggest that the number of CAPE environments generally increases, implying that unstable conditions become more frequent throughout Fennoscandia with a warming climate (Fig. 9). This is translated into relative increases in the area average occurrence of local CAPE environments (Fig. 5j–l), which is more pronounced in the north. In contrast, area average number of precipitating and DLS environments are projected to generally decrease or remain somewhat unchanged in Finland and Sweden, indicating that precipitation and strong shear may become less common overall

https://doi.org/10.5194/egusphere-2026-4247
Preprint. Discussion started: 22 July 2026

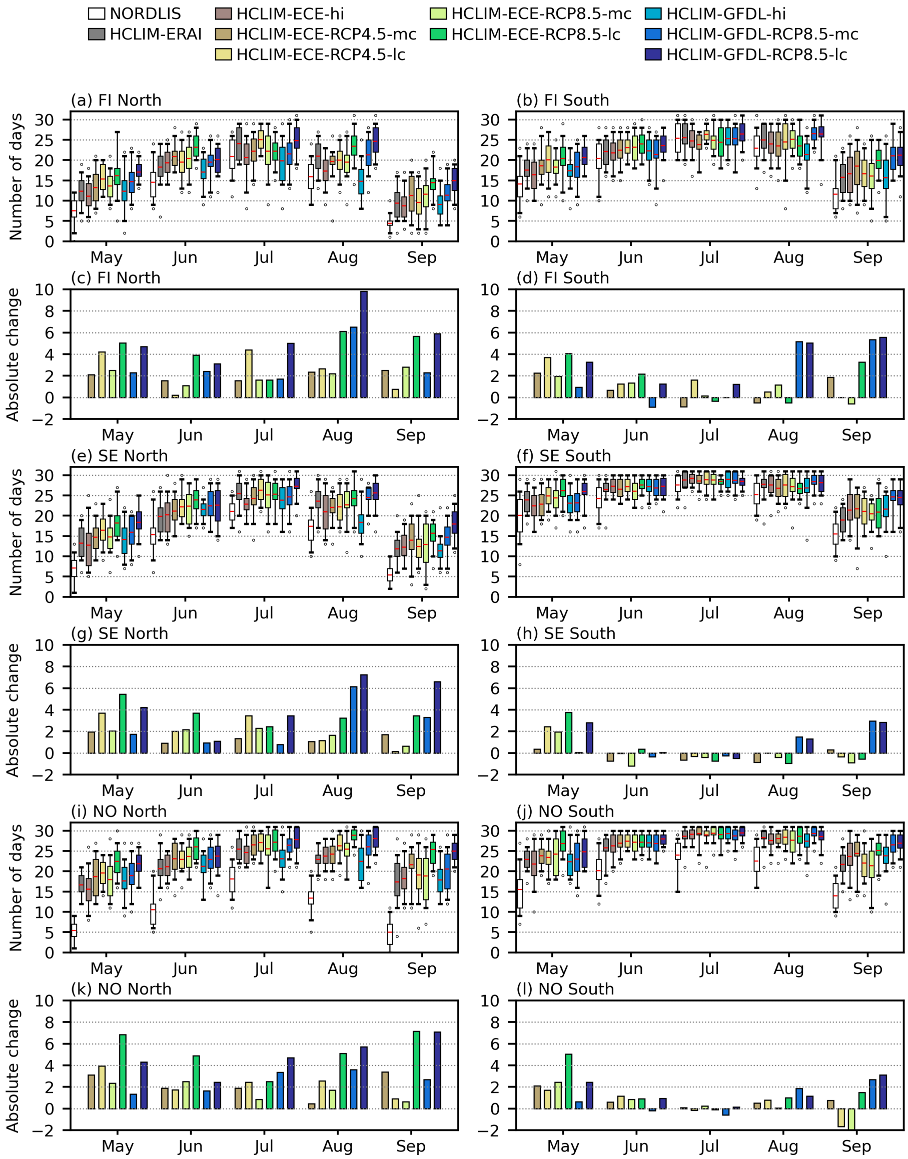

Figure 8. Monthly distribution of the regional number of days that meet the thunderstorm-environment criteria in HCLIM-ECE and HCLIM-GFDL for two subregions of Finland (a)–(b), Sweden (c)–(d), and Norway (e)–(f). Labels "hi", "mc", and "lc" denote the periods 1986–2005, 2041–2060, and 2081–2100, respectively. Corresponding values from the HCLIM-ERAI hindcast simulation and the observed regional thunder days from NORDLIS are shown for 2002–2018. Boxplots show interannual variability, with red solid line indicating the mean, boxes the 25th–75th percentiles, and whiskers the 1st–99th percentiles. Absolute changes in the annual mean are shown for Finland (c)–(d), Sweden (g)–(h), and Norway (k)–(l). Southern and northern regions are indicated by empty and hatched bars, respectively.

https://doi.org/10.5194/egusphere-2026-4247
Preprint. Discussion started: 22 July 2026

(Fig. 5m–n, p–q, see also Figs. 10–11). The response is more complex in Norway (Fig. 5o and r), namely, precipitation is projected to become more common along the Scandinavian mountain range (Fig. 10) and strong DLS occurrence is shown to increase in southern Norway (and parts of Sweden) in some simulations (Fig. 11).

It appears that the increase in the frequency of thunderstorm environments in Finland, Sweden and Norway is mainly the result of more numerous CAPE environments (Fig. 5j–l). The decreases in precipitating environments in Finland and Sweden overall do not offset the increase in CAPE. However, a part of the decrease in precipitating environments in Finland and Sweden seems to occur during unstable conditions (Fig. 5s–t), and the fraction of unstable environments that are also precipitating is simulated to decrease across most of Fennoscandia, at least according to HCLIM-GFDL-RCP8.5 (Fig. 5s–u).

Likewise, severe thunderstorm environments are projected to become more common mainly as a result of increased occurrence of unstable conditions (Fig. 5j–l), and the overall decrease in the frequency of strong shear environments is not able to offset the increase in CAPE environments (Fig. 5p–r). In Finland, the fraction of thunderstorm environments co-occurring with strong DLS is projected to decrease (most consistently in HCLIM-GFDL-RCP8.5, Fig. 5v), suggesting that the fraction of thunderstorm-favourable conditions capable of producing severe weather might decrease. The response is more complex in Sweden and Norway (Fig. 5w–x), although southern Norway exhibits quite consistent increases in the fraction of thunderstorm-environments that are also strongly sheared across simulations (Fig. 5x). This suggests that in southern Norway, strong DLS co-occurring with unstable and precipitating conditions might become more common (Fig. 5x).

5 Discussion

This study complements previous pan-European assessments of future thunderstorm environments that utilized an ensemble of regional EURO-CORDEX climate model simulations at approximately 50 km spatial resolution (Púčik et al., 2017; Rädler et al., 2019). The present work provides, for the first time, a regionally detailed assessment of the future projections of thunderstorm-favourable conditions in Fennoscandia during the main thunderstorm season (May–September). We use climate simulations specifically developed for the Fennoscandian region and show good performance of the model and applied proxies in replicating observed thunder day climate, which provides confidence in their applicability in the region.

The results from this study are generally in line with the EURO-CORDEX ensemble mean response reported by Púčik et al. (2017) using a similar threshold-based proxy. Namely, both project increased frequency of days with favourable conditions for the occurrence (severe) of thunderstorms. However, the response of individual environmental ingredients is more complex according to HCLIM than indicated by the EURO-CORDEX mean. While EURO-CORDEX simulations indicate increasing frequencies of precipitating environments and decreasing occurrences of strong DLS, the HCLIM simulations show a decrease in precipitation frequency across much of Finland and Sweden, but with increases over the Scandinavian mountains. Similarly, DLS decreases across most of Fennoscandia, but increases in southern Norway in some HCLIM simulations.

Despite these regional differences, the overall conclusion remains similar between the current and previous studies, namely, increases in convective instability are projected to be associated with a rise in (severe) thunderstorm-favourable conditions across Fennoscandia by the end of the 21st century. This leads to more numerous occurrences where the CAPE, precipitation

https://doi.org/10.5194/egusphere-2026-4247
Preprint. Discussion started: 22 July 2026

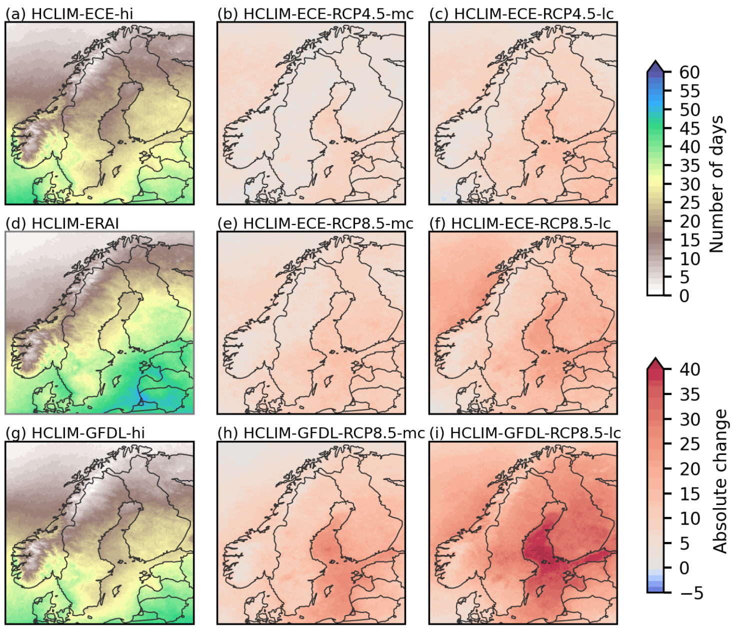

Figure 9. Seasonal (May–September) mean number of days with at least one occurrence of CAPE > 150 J kg^{-1} in (a) HCLIM-ECE-hi in the historical period (1986–2005), and its absolute change by mid-century (2041–2060) and late-century (2081–2100) under (b)–(c) HCLIM-ECE-RCP4.5 and (e)–(f) HCLIM-ECE-RCP8.5. Corresponding results for HCLIM-GFDL-hi and HCLIM-GFDL-RCP8.5 are shown in (g)–(i). Panel (d) shows the mean number of days from the HCLIM-ERAI hindcast (1998–2018).

and DLS criteria still co-occur, even in regions where the frequency of precipitation or strong shear decrease overall. The regional variations highlight detailed responses that may not be represented by pan-European studies with coarser models, and show the value of high-resolution models for regional climate change assessments.

The results from this study contain uncertainties arising from a few different issues. First, we utilize a single regional climate model, forced with two GCMs at the lateral boundaries. Therefore, we are not able to provide an uncertainty estimate for the level of projected change. The HCLIM-GCM-hi simulations exhibit biases (Lind et al., 2023), that translate into differences in the frequency of storm environments compared to the HCLIM-ERAI hindcast simulation.

Second, we utilize simple threshold-based proxies that depend only on the presence of CAPE, DLS and precipitation, while the formation of lightning and other specific surface hazards requires more numerous factors and complex interactions that are not taken into account. While the applied precipitation threshold increases the likelihood of convective initiation under unstable conditions, it does not ensure that the precipitation is associated with a convective storm or that lightning occurs, and the proxies may occasionally capture non-convective precipitation.

Dry environmental air in the low-to-mid troposphere around convective updrafts or stable layers in the lower troposphere (i.e. large CIN) may limit the growth of convective clouds or inhibit storm formation by reducing parcel buoyancy even if CAPE is present. ERA5-based studies have indicated that over Fennoscandia in the last decades, median 0–4 km relative humidity

https://doi.org/10.5194/egusphere-2026-4247
Preprint. Discussion started: 22 July 2026

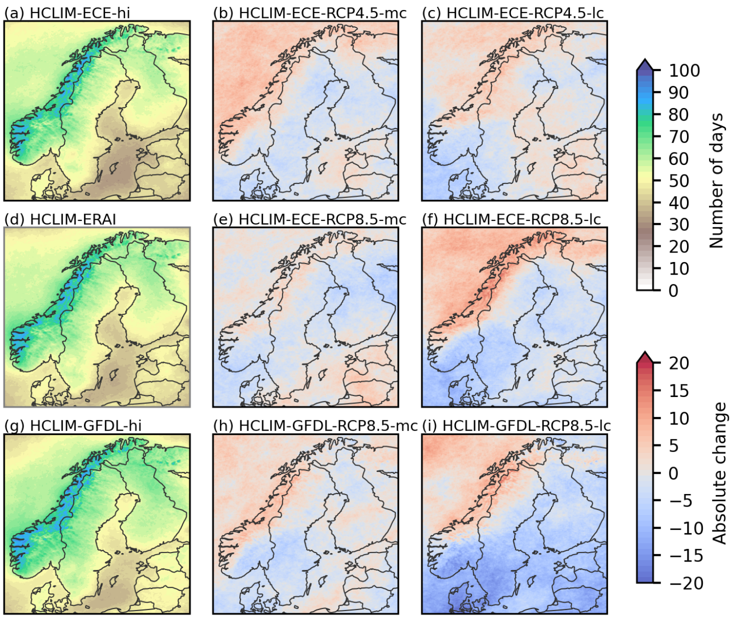

Figure 10. Seasonal (May–September) mean number of days with at least one occurrence of 3-hourly precipitation > 0.5 mm in (a) HCLIM-ECE-hi in the historical period (1986–2005), and its absolute change by mid-century (2041–2060) and late-century (2081–2100) under (b)–(c) HCLIM-ECE-RCP4.5 and (e)–(f) HCLIM-ECE-RCP8.5. Corresponding results for HCLIM-GFDL-hi and HCLIM-GFDL-RCP8.5 are shown in (g)–(i). Panel (d) shows the mean number of days from the HCLIM-ERAI hindcast (1998–2018).

(RH) during unstable conditions has decreased slightly, while the fraction of inhibiting (CIN > 75 J kg^{-1}) environments from unstable environments has remained largely unchanged (Taszarek et al., 2021a). The focus of this study is on changes in CAPE, DLS and precipitation, however, brief sensitivity test to CIN and RH was conducted. According to HCLIM in both the historical and future periods, days with dry (700 hPa RH < 50 %) or inhibiting (CIN > 75 J kg^{-1}) conditions in Finland, Sweden and Norway occur only on a small fraction (approximately 0–0.2) of thunderstorm-favourable days (see Figs. A3–A4). Slight increases in the fraction of inhibiting environments (Fig. A4) are projected due to overall (not shown) increased occurrence of days with CIN > 75 J kg^{-1}. Changes in the fraction of dry environments are less consistent (Fig. A3). However, RH is evaluated at a single pressure level and might be influenced by ongoing convection, and CIN is derived from relatively coarse model output, making the effect of changes in mid-tropospheric RH and CIN on storm-favourable environments uncertain.

Lastly, the occurrence of a favourable environment is defined by applying single fixed thresholds for convective parameters, whereas in reality, there are no universal thresholds for CAPE or DLS with which the occurrence of a (severe) storm would be guaranteed (Doswell and Schultz, 2006). Thus, the number of favourable environments is inevitably sensitive to the thresholds applied. For example, lowering the DLS threshold from 12.5 m s^{-1} to 10 m s^{-1}, as in Taszarek et al. (2021a), or raising it to 15 m s^{-1}, as in Púčik et al. (2017), results in slightly more or fewer detected severe thunderstorm environments, respectively (not shown). However, the distributions of storm environments remain similar if the thresholds for proxy parameters are slightly

https://doi.org/10.5194/egusphere-2026-4247
Preprint. Discussion started: 22 July 2026

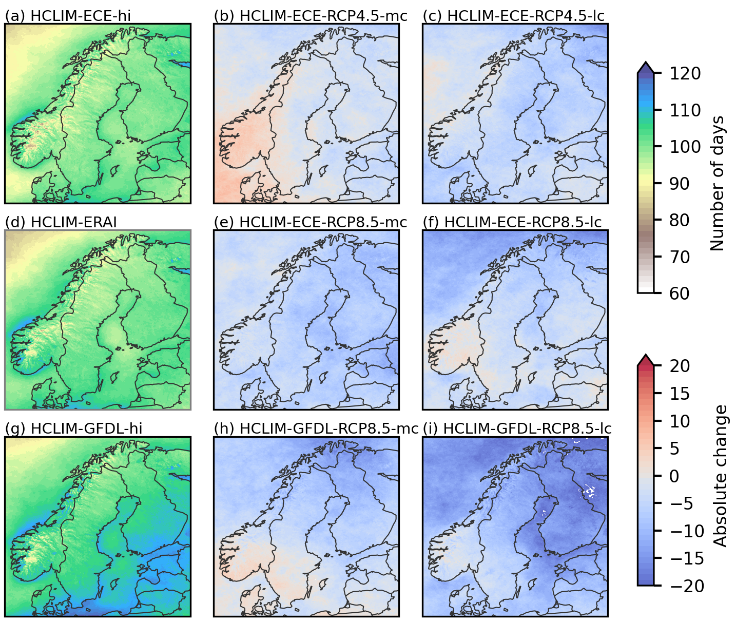

Figure 11. Seasonal (May–September) mean number of days with at least one occurrence of DLS > 12.5 m s^{-1} in (a) HCLIM-ECE-hi in the historical period (1986–2005), and its absolute change by mid-century (2041–2060) and late-century (2081–2100) under (b)–(c) HCLIM-ECE-RCP4.5 and (e)–(f) HCLIM-ECE-RCP8.5. Corresponding results for HCLIM-GFDL-hi and HCLIM-GFDL-RCP8.5 are shown in (g)–(i). Panel (d) shows the mean number of days from the HCLIM-ERAI hindcast (1998–2018).

increased or decreased (not shown). Nevertheless, tuning the thresholds so that the frequency of favourable environments corresponds to observed events may also not be meaningful, since differences may arise simply from other known limitations (e.g. missing ingredients and model biases).

Despite these limitations, we show that HCLIM agrees well with ERA5 in terms of the distributions of individual proxy components. Furthermore, the proxies and thresholds are physically justifiable and have been applied in previous studies on other datasets (Taszarek et al., 2019, 2021a; Púčik et al., 2017). HCLIM and the proxies indicate highest potential for (severe) thunderstorm occurrence in regions with most frequent observed lightning and the number of thunderstorm-favourable days is the same order of magnitude as observed thunder days in Fennoscandia. Therefore, the proxies appear to be useful in assessing how the conditions that increase the likelihood for storm occurrence might change as the climate warms. However, we note that our proxy performance appear to be region-dependent. Results over the Scandinavian mountain range should be interpreted with caution, as also noted by Taszarek et al. (2019).

While this study indicates increases in the number of conditions supporting (severe) thunderstorms, it remains unclear how the changes translate into changes in the actual occurrences of convective storms. One possible way forward is to assign probabilities of hazard occurrence as functions of a wider set of environmental parameters, which may yield more robust estimates for specific hazards. The use of a convection-permitting climate model also offers the potential to analyze process-based model

https://doi.org/10.5194/egusphere-2026-4247
Preprint. Discussion started: 22 July 2026

diagnostics and storm-scale constraints of hazard formation rather than relying solely on environmental indicators. However, even when deep convection is explicitly resolved, the estimated changes still contain uncertainties arising from parameterizations of subgrid-scale processes and limited output resolution. Moreover, producing reliable probabilities of local impacts using model data requires observational data for proxy development and model evaluation. In Fennoscandia, publications on the climatology of severe convection are limited and observational datasets contain spatial and temporal inhomogeneities due to underreporting in large uninhabited areas (Rauhala et al., 2012; Groenemeijer et al., 2017; Virman et al., 2025).

6 Conclusions

This study explores the future scenarios of environmental conditions favourable for the occurrence of (severe) thunderstorms in Fennoscandia during the thunderstorm season in May–September. The analysis was conducted using kilometer-scale simulations made with the convection-permitting regional climate model HCLIM, forced with two GCMs with different climate change signals at the lateral boundaries and under projected RCP4.5 and RCP8.5 greenhouse gas concentration scenarios. Thunderstorm-favourable days were defined from 3-hourly model output using simple fixed-threshold-based proxies that combine model simulated instantaneous CAPE (measure of conditional instability and good indicator for lightning) and 3-hourly precipitation (proxy for convective initiation). Severe thunderstorm-favourable days were defined analogously, but with an additional requirement for strong DLS that is linked with organized severe convection.

HCLIM and the storm proxies indicate most frequent unstable conditions and highest potential for (severe) thunderstorms in the southern regions of Finland, Sweden and Norway. The general spatial pattern of (severe) thunderstorm-favourable days in the historical HCLIM simulations corresponds qualitatively with observed thunder days, except in the case of southwestern Norway, where HCLIM shows a more robust maximum. The absolute numbers of storm-favourable days in the historical HCLIM simulations slightly differ from observations due to model biases and simplified proxy assumptions. Despite this limitation, the overall good correspondence suggests that the proxy can identify regions with higher storm likelihood and be used to assess future changes.

Increasing greenhouse gas concentrations are projected to lead to more frequent conditions favourable for (severe) thunderstorms across much of Fennoscandia, with changes already apparent by mid-century (2041–2060) and strengthening further towards the end of the century (2081–2100). By the end of the century, the area-average occurrence of thunderstorm-favourable days is projected to increase by approximately 40–185 % in Finland, 30–185 % in Sweden, and 15–210 % in Norway. The relative increase is generally larger in the northern half of the countries where storm-environments and thunder days are fewer than in the southern regions. Increases are consistently stronger under RCP8.5 than RCP4.5, and in HCLIM-GFDL (strong warming) compared to HCLIM-ECE (close to CMIP5 ensemble mean warming response). We note that while RCP8.5 is generally considered less likely than RCP4.5, it remains useful for assessing responses to strong warming. According to HCLIM, the increases in (severe) thunderstorm-favourable days appear to be primarily driven by an increasing frequency of unstable conditions.

https://doi.org/10.5194/egusphere-2026-4247
Preprint. Discussion started: 22 July 2026

In addition to increases in area-average occurrences, the annual mean number of regional thunderstorm-favourable days (defined as days with at least one proxy occurrence anywhere in the region) is expected to rise in the northern regions of Fennoscandia, with changes distributed throughout May–September. This suggests that in the north, future favourable conditions may become both more frequent and more widespread. In the south, however, only small increases in the regional occurrence are projected and mainly outside the peak season (June–July–August), suggesting that the average number of thunderstorm-favourable days overall may not increase much. Despite the smaller projected changes, the southern regions continue to experience more (severe) thunderstorm-favourable days than northern regions, both locally and regionally, in the future simulations. Furthermore, the large interannual and monthly variability observed in the historical period and for observed thunder days is projected to persist under climate change.

This study has some limitations (discussed in Sect. 5). Most notably, the results are based on a single regional climate model and therefore represent only one possible climate change pathway. Furthermore, the changes in storm-favourable conditions are based on proxies that simplify the relationship between the atmospheric conditions and thunderstorm occurrence. While the proxy for thunderstorm environment is able to reproduce the general spatial distribution of observed thunder days, it is unclear if the same is true for severe environments, and the performance of the proxies are region dependent. Thus, the projections should be interpreted with caution, especially over complex terrain, such as much of Norway.

There is an increasing need for better understanding of how the occurrence and intensity of convective storms, especially the damaging ones, might evolve in a warming climate. This study shows increases in environmental conditions favourable for the development of (severe) thunderstorms using simple threshold-based proxies. However, it remains unclear how these changes translate into changes in the probability of lightning, wind gusts, hail or other convective hazards. Future work will explore the long-term occurrence of damaging convection in Fennoscandia by utilizing impact-based data and will develop more specific proxies for hazard occurrence in high-resolution datasets. These efforts will provide more detailed estimates of climate change impacts and support climate adaptation and risk preparedness across sectors.

Data availability. The HCLIM and ERA5 data were downloaded from the NIRD Research Data Archive (The HARMONIE Climate community, 2025a, b, c, d) and Climate Data Store (Hersbach et al., 2023b, a), respectively. The NORDLIS lightning location data is available from the Open Data Service of the Finnish Meteorological Institute at https://en.ilmatieteenlaitos.fi/open-data.

Author contributions. M.V. conceptualized and designed the study, performed the analysis, and prepared the visualizations. A.L. contributed to the conceptual framing of the research theme. A.M. processed and provided the lightning data. T.K.L. validated the analysed model data. P.L. produced and validated the original model data. M.V. wrote the original draft of the manuscript. A.M. T.K.L., P.L. and A.L. contributed to reviewing and editing the manuscript. H.G. acquired the funding.

Competing interests. The contact author has declared that none of the authors has any competing interests.

Acknowledgements. The HCLIM data were produced by the NorCP project, a Nordic collaboration involving climate modeling groups from the Danish Meteorological Institute (DMI), Finnish Meteorological Institute (FMI), Norwegian Meteorological Institute (MET Norway), and Swedish Meteorological and Hydrological Institute (SMHI). We thank CSC – IT Center for Science for providing the computational resources used in this analysis. This study was funded by the European Union's Horizon Europe research and innovation programme through the PIISA project (Piloting Innovative Insurance Solutions for Adaptation, Grant Agreement No. 101112841), by the Finnish State Nuclear

https://doi.org/10.5194/egusphere-2026-4247
Preprint. Discussion started: 22 July 2026

Waste Management Fund (VYR) through the MAWECLI2 project (Dnro SAFER 5/2026) in the SAFER2028 programme by the Postdoctoral Programme for Research Institutes in Finland, funded by the Finnish Government.

540 ## Appendix A

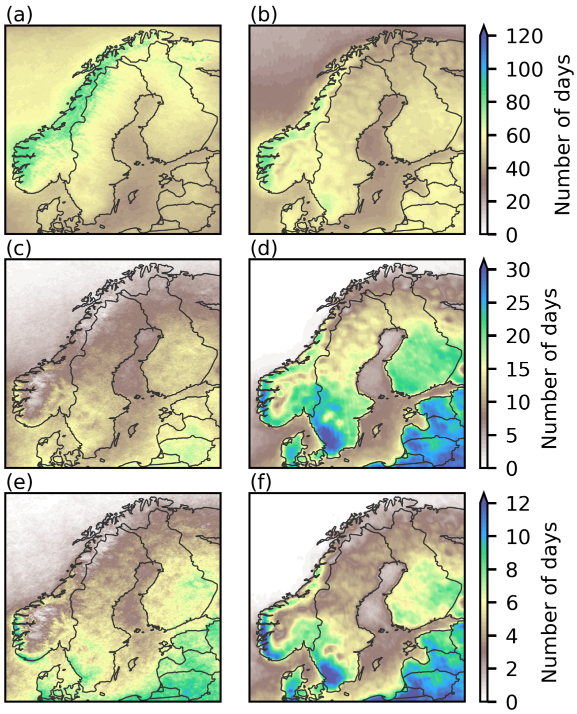

Figure A1. Seasonal (May–September) mean number of days with at least one occurrence of (a)–(b) 3-hourly precipitation > 0.5 mm, and days that meet the criteria for (c)–(d) thunderstorm environment and (e)–(f) severe thunderstorm environment in HCLIM-ERAI (left column) and ERA5 (right column) in 1998–2018. Note that in (b), (d) and (f), precipitation includes only the convective precipitation component. Both datasets are in their native grid.

https://doi.org/10.5194/egusphere-2026-4247
Preprint. Discussion started: 22 July 2026

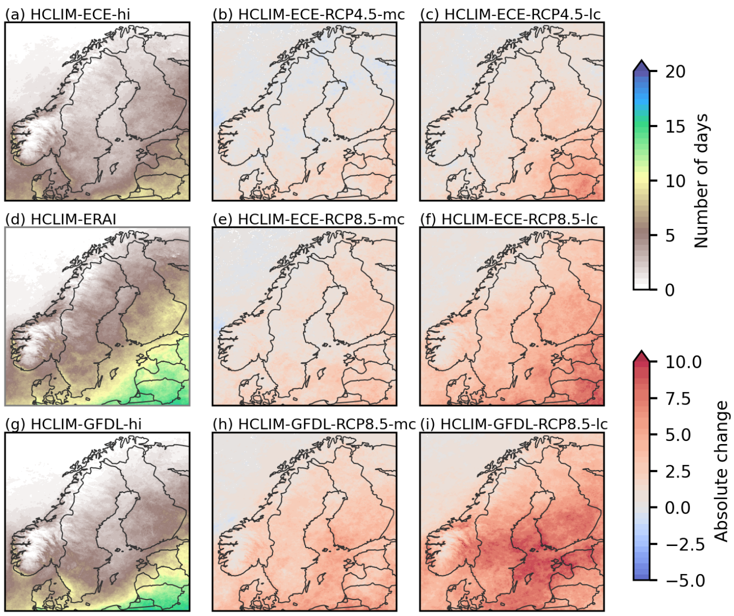

Figure A2. Seasonal (May–September) mean number of days that meet the criteria for CAPESHEAR environment in (a) HCLIM-ECE-hi in 1986–2005, and its absolute change by mid-century (2041–2060) and late-century (2081–2100) under (b)–(c) HCLIM-ECE-RCP4.5 and (e)–(f) HCLIM-ECE-RCP8.5. Corresponding results for HCLIM-GFDL-hi and HCLIM-GFDL-RCP8.5 are shown in (g)–(i). Panel (d) shows the mean number of days from the HCLIM-ERAI hindcast (1998–2018).

https://doi.org/10.5194/egusphere-2026-4247
Preprint. Discussion started: 22 July 2026

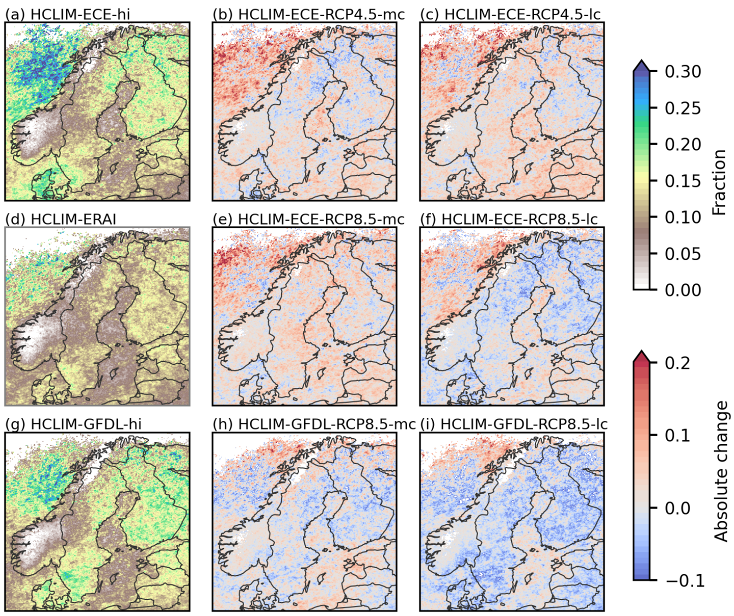

Figure A3. Seasonal (May–September) mean fraction of days per year that meet the criteria for thunderstorm environments occurring simultaneously with 700 hPa relative humidity $<$ 50 % from thunderstorm environments in (a) HCLIM-ECE-hi in 1986–2005, and its absolute change by mid-century (2041–2060) and late-century (2081–2100) under (b)–(c) HCLIM-ECE-RCP4.5 and (e)–(f) HCLIM-ECE-RCP8.5. Corresponding results for HCLIM-GFDL-hi and HCLIM-GFDL-RCP8.5 are shown in (g)–(i). Panel (d) shows the mean fraction from the HCLIM-ERAI hindcast (1998–2018).

https://doi.org/10.5194/egusphere-2026-4247
Preprint. Discussion started: 22 July 2026

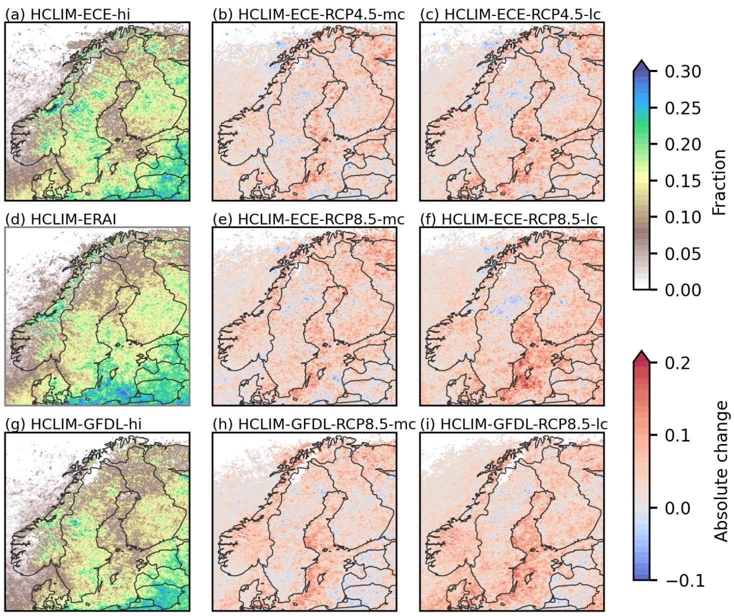

Figure A4. Seasonal (May–September) mean fraction of days per year that meet the criteria for thunderstorm environments occurring simultaneously with CIN > 75 J kg^{-1} from thunderstorm environments in (a) HCLIM-ECE-hi in 1986–2005, and its absolute change by mid-century (2041–2060) and late-century (2081–2100) under (b)–(c) HCLIM-ECE-RCP4.5 and (e)–(f) HCLIM-ECE-RCP8.5. Corresponding results for HCLIM-GFDL-hi and HCLIM-GFDL-RCP8.5 are shown in (g)–(i). Panel (d) shows the mean fraction from the HCLIM-ERAI hindcast (1998–2018).

https://doi.org/10.5194/egusphere-2026-4247
Preprint. Discussion started: 22 July 2026

References

Allen, J. T.: Climate Change and Severe Thunderstorms, in: Oxford Research Encyclopedia of Climate Science, edited by von Storch, H., Oxford University Press, ISBN 9780197851746, https://doi.org/10.1093/acrefore/9780190228620.013.62, 2018.

An, D., Olsson, J., Du, Y., Sörensen, J., Uvo, C. B., and Berg, P.: Future projections of wet and dry spells in southern Sweden: The impact of climate model resolution, Atmos. Res., 330, 108 547, https://doi.org/h10.1016/j.atmosres.2025.108547, 2026.

Antonescu, B., Schultz, D. M., Lomas, F., and Kühne, T.: Tornadoes in Europe: Synthesis of the observational datasets, Mon. Weather Rev., 144, 2445–2480, https://doi.org/10.1175/MWR-D-15-0298.1, 2016.

Battaglioli, F., Taszarek, M., Groenemeijer, P., Púčik, T., and Rädler, A.: Contrasting trends in very large hail events and related economic losses across the globe, Nat. Geosci., 19, 52–58, https://doi.org/10.1038/s41561-025-01868-0, 2026.

Bechtold, P., Semane, N., Lopez, P., Chaboureau, J.-P., Beljaars, A., and Bormann, N.: Representing equilibrium and nonequilibrium convection in large-scale models, J. Atmos. Sci., 71, 734–753, https://doi.org/10.1175/JAS-D-13-0163.1, 2014.

Belušić, D., de Vries, H., Dobler, A., et al.: HCLIM38: a flexible regional climate model applicable for different climate zones from coarse to convection-permitting scales, Geosci. Model Dev., 13, 1311–1333, https://doi.org/10.5194/gmd-13-1311-2020, 2020.

Bengtsson, L., Andrae, U., Aspelien, T., et al.: The HARMONIE–AROME Model Configuration in the ALADIN–HIRLAM NWP System, Mon. Weather Rev., 145, 1919–1935, https://doi.org/10.1175/MWR-D-16-0417.1, 2017.

Brisson, E., Blahak, U., Lucas-Picher, P., Purr, C., and Ahrens, B.: Contrasting lightning projection using the lightning potential index adapted in a convection-permitting regional climate model, Clim. Dynam., 57, 2037–2051, https://doi.org/10.1007/s00382-021-05791-z, 2021.

Brooks, H. E.: Severe thunderstorms and climate change, Atmos. Res., 123, 129–138, https://doi.org/10.1016/j.atmosres.2012.04.002, 2013.

Brooks, H. E., Lee, J. W., and Craven, J. P.: The spatial distribution of severe thunderstorm and tornado environments from global reanalysis data, Atmos. Res., 67, 73–94, https://doi.org/10.1016/S0169-8095(03)00045-0, 2003.

Brown, A., Dowdy, A., and Lane, T. P.: Convection-permitting climate model representation of severe convective wind gusts and future changes in southeastern Australia, Nat. Hazards Earth Syst. Sci., 24, 3225–3243, https://doi.org/10.5194/nhess-24-3225-2024, 2024.

Cui, R., Thurnherr, I., Velasquez, P., Brennan, K., Leclair, M., Mazzoleni, A., Schmid, T., Wernli, H., and Schär, C.: A European hail and lightning climatology from an 11-year kilometer-scale regional climate simulation, J. Geophys. Res. Atmos., 130, e2024JD042 828, https://doi.org/10.1029/2024JD042828, 2025.

Cui, W., Hoogewind, K. A., and Galarneau Jr, T. J.: A climatology of mesoscale convective system hazards in the United States and their representation in a convection-permitting model, J. Geophys. Res. Atmos., 131, e2025JD045 335, https://doi.org/10.1029/2025JD045335, 2026.

Dee, D. P., Uppala, S. M., Simmons, A. J., et al.: The ERA-Interim reanalysis: configuration and performance of the data assimilation system, Quart. J. Roy. Meteorol. Soc., 137, 553–597, https://doi.org/10.1002/qj.828, 2011.

Diffenbaugh, N. S., Scherer, M., and Trapp, R. J.: Robust increases in severe thunderstorm environments in response to greenhouse forcing, Proc. Nat. Acad. Sci. USA, 110, 16 361–16 366, https://doi.org/10.1073/pnas.1307758110, 2013.

Donner, L. J., Wyman, B. L., Hemler, R. S., Horowitz, L. W., Ming, Y., Zhao, M., Golaz, J.-C., Ginoux, P., Lin, S.-J., Schwarzkopf, M. D., et al.: The dynamical core, physical parameterizations, and basic simulation characteristics of the atmospheric component AM3 of the GFDL global coupled model CM3, J. Climate, 24, 3484–3519, https://doi.org/10.1175/2011JCLI3955.1, 2011.

Doswell, C. A. I. and Schultz, D. M.: On the use of indices and parameters in forecasting severe storms, E-Journal of Severe Storms Meteorology, 1, 1–22, https://doi.org/10.55599/ejssm.v1i3.4, 2006.

https://doi.org/10.5194/egusphere-2026-4247
Preprint. Discussion started: 22 July 2026

Doswell, C. A. I., Brooks, H. E., and Maddox, R. A.: Flash flood forecasting: An ingredients-based methodology, Weather Forecast., 11, 560–581, https://doi.org/10.1175/1520-0434(1996)011<0560:FFFAIB>2.0.CO;2, 1996.

Dyrrdal, A. V., Olsson, J., Médus, E., Arnbjerg-Nielsen, K., Post, P., Aņiskeviča, S., Thorndahl, S., Førland, E., Wern, L., Mačiulytė, V., et al.: Observed changes in heavy daily precipitation over the Nordic-Baltic region, J. Hydrol. Reg. Stud., 38, 100 965, https://doi.org/10.1016/j.ejrh.2021.100965, 2021.

Enno, S.-E., Sugier, J., Alber, R., and Seltzer, M.: Lightning flash density in Europe based on 10 years of ATDnet data, Atmos. Res., 235, 104 769, https://doi.org/10.1016/j.atmosres.2019.104769, 2020.

Groenemeijer, P., Púčik, T., Holzer, A. M., Antonescu, B., Riemann-Campe, K., Schultz, D. M., Kühne, T., Feuerstein, B., Brooks, H. E., Doswell, C. A. I., et al.: Severe convective storms in Europe: Ten years of research and education at the European Severe Storms Laboratory, Bull. Amer. Meteorol. Soc., 98, 2641–2651, https://doi.org/10.1175/BAMS-D-16-0067.1, 2017.

Hazeleger, W., Wang, X., Severijns, C., Ştefănescu, S., Bintanja, R., Sterl, A., Wyser, K., Semmler, T., Yang, S., Van den Hurk, B., et al.: EC-Earth V2. 2: description and validation of a new seamless earth system prediction model, Clim. Dynam., 39, 2611–2629, https://doi.org/10.1007/s00382-011-1228-5, 2012.

Hersbach, H., Bell, B., Berrisford, P., et al.: The ERA5 global reanalysis, Quart. J. Roy. Meteorol. Soc., 146, 1999–2049, https://doi.org/10.1002/qj.3803, 2020.

Hersbach, H., Bell, B., Berrisford, P., Biavati, G., Horányi, A., Muñoz Sabater, J., Nicolas, J., Peubey, C., Radu, R., Rozum, I., Schepers, D., Simmons, A., Soci, C., Dee, D., and Thépaut, J.-N.: ERA5 hourly data on pressure levels from 1940 to present, Copernicus Climate Change Service (C3S) Climate Data Store (CDS), https://doi.org/10.24381/cds.bd0915c6, accessed on 25-Jun-2026, 2023a.

Hersbach, H., Bell, B., Berrisford, P., Biavati, G., Horányi, A., Muñoz Sabater, J., Nicolas, J., Peubey, C., Radu, R., Rozum, I., Schepers, D., Simmons, A., Soci, C., Dee, D., and Thépaut, J.-N.: ERA5 hourly data on single levels from 1940 to present, Copernicus Climate Change Service (C3S) Climate Data Store (CDS), https://doi.org/10.24381/cds.adbb2d47, accessed on 25-Jun-2026, 2023b.

Kahraman, A., Kendon, E. J., Fowler, H. J., and Short, C. J.: Future changes in severe hail across Europe, including regional emergence of warm-type thunderstorms, Nat. Commun., 16, 8438, https://doi.org/10.1038/s41467-025-62780-0, 2025.

Lind, P., Belušić, D., Christensen, O. B., Dobler, A., Kjellström, E., Landgren, O., et al.: Benefits and Added Value of Convection-Permitting Climate Modeling over Fenno-Scandinavia, Clim. Dynam., 55, 1893–1912, https://doi.org/10.1007/s00382-020-05359-3, 2020.

Lind, P., Belušić, D., Médus, E., Dobler, A., Pedersen, R. A., Wang, F., Matte, D., Kjellström, E., Landgren, O., Lindstedt, D., et al.: Climate change information over Fenno-Scandinavia produced with a convection-permitting climate model, Clim. Dynam., 61, 519, https://doi.org/10.1007/s00382-022-06589-3, 2023.

Lindstedt, D., Lind, P., Kjellström, E., and Jones, C.: A new regional climate model operating at the meso-gamma scale: performance over Europe, Tellus B, https://doi.org/10.3402/tellusa.v67.24138, 2015.

Lucas-Picher, P., Argüeso, D., Brisson, E., Tramblay, Y., Berg, P., Lemonsu, A., Kotlarski, S., and Caillaud, C.: Convection-permitting modeling with regional climate models: Latest developments and next steps, Wiley Interdiscip. Rev. Clim. Change, 12, e731, https://doi.org/10.1002/wcc.731, 2021.

Mäkelä, A., Enno, S.-E., and Haapalainen, J.: Nordic Lightning Information System: Thunderstorm climate of northern Europe for the period 2002–2011, Atmos. Res., 139, 46–61, https://doi.org/10.1016/j.atmosres.2014.01.008, 2014.

Moss, R. H., Edmonds, J. A., Hibbard, K. A., Manning, M. R., Rose, S. K., Van Vuuren, D. P., Carter, T. R., Emori, S., Kainuma, M., Kram, T., et al.: The next generation of scenarios for climate change research and assessment, Nature, 463, 747–756, https://doi.org/10.1038/nature08823, 2010.

Médus, E., Thomassen, E. D., Belušić, D., Lind, P., Berg, P., Christensen, J. H., et al.: Characteristics of precipitation extremes over the Nordic region: added value of convection-permitting modeling, Nat. Hazards Earth Syst. Sci., 22, 693–711, https://doi.org/10.5194/nhess-22-693-2022, 2022.

Púčik, T., Groenemeijer, P., Rỳva, D., and Kolář, M.: Proximity soundings of severe and nonsevere thunderstorms in central Europe, Mon. Weather Rev., 143, 4805–4821, https://doi.org/10.1175/MWR-D-15-0104.1, 2015.

Púčik, T., Groenemeijer, P., Rädler, A. T., Tijssen, L., Nikulin, G., Prein, A. F., van Meijgaard, E., Fealy, R., Jacob, D., and Teichmann, C.: Future changes in European severe convection environments in a regional climate model ensemble, J. Climate, 30, 6771–6794, https://doi.org/10.1175/JCLI-D-16-0777.1, 2017.

Punkka, A.-J. and Bister, M.: Mesoscale convective systems and their synoptic-scale environment in Finland, Weather Forecast., 30, 182–196, https://doi.org/10.1175/WAF-D-13-00146.1, 2015.

Punkka, A.-J., Teittinen, J., and Johns, R. H.: Synoptic and mesoscale analysis of a high-latitude derecho–severe thunderstorm outbreak in Finland on 5 July 2002, Weather Forecast., 21, 752–763, https://doi.org/10.1175/WAF953.1, 2006.

Rädler, A. T., Groenemeijer, P., Faust, E., and Sausen, R.: Detecting severe weather trends using an additive regressive convective hazard model (AR-CHaMo), J. Appl. Meteorol. Climatol., 57, 569–587, https://doi.org/10.1175/JAMC-D-17-0132.1, 2018.

Rädler, A. T., Groenemeijer, P. H., Faust, E., Sausen, R., and Púčik, T.: Frequency of severe thunderstorms across Europe expected to increase in the 21st century due to rising instability, npj Clim. Atmos. Sci., 2, 30, https://doi.org/10.1038/s41612-019-0083-7, 2019.

Rantala, O., Räisänen, J., Rauhala, J., and Bister, M.: Derecho-favoring atmospheric environments in Finland: characteristics, identification criteria, and increasing frequency, eGUsphere [preprint], 2026.

Rauhala, J., Brooks, H. E., and Schultz, D. M.: Tornado climatology of Finland, Mon. Weather Rev., 140, 1446–1456, https://doi.org/10.1175/MWR-D-11-00196.1, 2012.

Taszarek, M., Brooks, H. E., and Czernecki, B.: Sounding-derived parameters associated with convective hazards in Europe, Mon. Weather Rev., 145, 1511–1528, https://doi.org/10.1175/MWR-D-16-0384.1, 2017.

Taszarek, M., Allen, J., Púčik, T., Groenemeijer, P., Czernecki, B., Kolendowicz, L., Lagouvardos, K., Kotroni, V., and Schulz, W.: A climatology of thunderstorms across Europe from a synthesis of multiple data sources, J. Climate, 32, 1813–1837, https://doi.org/10.1175/JCLI-D-18-0372.1, 2019.

Taszarek, M., Allen, J. T., Groenemeijer, P., Edwards, R., Brooks, H. E., Chmielewski, V., and Enno, S.-E.: Severe convective storms across Europe and the United States. Part I: Climatology of lightning, large hail, severe wind, and tornadoes, J. Climate, 33, 10 239–10 261, https://doi.org/10.1175/JCLI-D-20-0345.1, 2020a.

Taszarek, M., Kendzierski, S., and Pilguj, N.: Hazardous weather affecting European airports: Climatological estimates of situations with limited visibility, thunderstorm, low-level wind shear and snowfall from ERA5, Weather Clim. Extremes, 28, 100 243, https://doi.org/10.1016/j.wace.2020.100243, 2020b.

Taszarek, M., Allen, J. T., Brooks, H. E., Pilguj, N., and Czernecki, B.: Differing Trends in United States and European Severe Thunderstorm Environments in a Warming Climate, Bull. Amer. Meteorol. Soc., 102, E296 – E322, https://doi.org/10.1175/BAMS-D-20-0004.1, 2021a.

Taszarek, M., Allen, J. T., Marchio, M., and Brooks, H. E.: Global climatology and trends in convective environments from ERA5 and rawinsonde data, npj Clim. Atmos. Sci., 4, 35, https://doi.org/10.1038/s41612-021-00190-x, 2021b.

Taszarek, M., Pilguj, N., Allen, J. T., Gensini, V., Brooks, H. E., and Szuster, P.: Comparison of convective parameters derived from ERA5 and MERRA-2 with rawinsonde data over Europe and North America, J. Climate, 34, 3211–3237, https://doi.org/10.1175/JCLI-D-20-0484.1, 2021c.

https://doi.org/10.5194/egusphere-2026-4247
Preprint. Discussion started: 22 July 2026

The HARMONIE Climate community: NorCP HCLIM 3km EC-Earth RCP8.5 data, https://doi.org/10.11582/2025.V5H1QKWP, 2025a.

The HARMONIE Climate community: NorCP HCLIM 3km EC-Earth RCP4.5 data, https://doi.org/10.11582/2025.9Q7CJMS0, 2025b.

The HARMONIE Climate community: NorCP HCLIM 3km ERA-Interim data, https://doi.org/10.11582/2025.00064, 2025c.

The HARMONIE Climate community: NorCP HCLIM 3km GFDL-CM3 RCP8.5 data, https://doi.org/10.11582/2025.LAIXK5J6, 2025d.

Toll, V., Männik, A., Luhamaa, A., and Rõõm, R.: Hindcast experiments of the derecho in Estonia on 08 August, 2010: Modelling derecho with NWP model HARMONIE, Atmos. Res., 158-159, 179–191, https://doi.org/10.1016/j.atmosres.2014.10.011, 2015.

Torralba, V., Hénin, R., Cantelli, A., Scoccimarro, E., Materia, S., Manzato, A., and Gualdi, S.: Modelling hail hazard over Italy with ERA5 large-scale variables, Weather Clim. Extremes, 39, 100 535, https://doi.org/10.1016/j.wace.2022.100535, 2023.

Trapp, R. J., Diffenbaugh, N. S., Brooks, H. E., Baldwin, M. E., Robinson, E. D., and Pal, J. S.: Changes in severe thunderstorm environment frequency during the 21st century caused by anthropogenically enhanced global radiative forcing, Proc. Nat. Acad. Sci. USA, 104, 19 719–19 723, https://doi.org/10.1073/pnas.0705494104, 2007.

Trapp, R. J., Diffenbaugh, N. S., and Gluhovsky, A.: Transient response of severe thunderstorm forcing to elevated greenhouse gas concentrations, Geophys. Res. Lett., 36, https://doi.org/10.1029/2008GL036203, 2009.

Tsonevsky, I., Doswell, C. A. I., and Brooks, H. E.: Early warnings of severe convection using the ECMWF extreme forecast index, Weather Forecast., 33, 857–871, https://doi.org/10.1175/WAF-D-18-0030.1, 2018.

Tuovinen, J.-P., Punkka, A.-J., Rauhala, J., Hohti, H., and Schultz, D. M.: Climatology of severe hail in Finland: 1930–2006, Mon. Weather Rev., 137, 2238–2249, https://doi.org/10.1175/2008MWR2707.1, 2009.

Tuovinen, J.-P., Rauhala, J., and Schultz, D. M.: Significant-hail-producing storms in Finland: Convective-storm environment and mode, Weather Forecast., 30, 1064–1076, https://doi.org/10.1175/WAF-D-14-00159.1, 2015.

Ukkonen, P., Manzato, A., and Mäkelä, A.: Evaluation of thunderstorm predictors for Finland using reanalyses and neural networks, J. Appl. Meteorol. Climatol., 56, 2335–2352, https://doi.org/10.1175/JAMC-D-16-0361.1, 2017.

Utriainen, L., Virman, M., Laakso, A., Ritvanen, J., Jylhä, K., Merikanto, J., et al.: Less frequent but more intense summertime precipitation in Finland: results from a convection-permitting climate model, Boreal Environ. Res., 30, 93–109, https://doi.org/10.60910/ber2025.xv04-3n48, 2025.

Van Vuuren, D. P., Edmonds, J., Kainuma, M., Riahi, K., Thomson, A., Hibbard, K., Hurtt, G. C., Kram, T., Krey, V., Lamarque, J.-F., et al.: The representative concentration pathways: an overview, Clim. Change, 109, 5, https://doi.org/10.1007/s10584-011-0148-z, 2011.

Virman, M., Rantanen, M., Laurila, T. K., Mäkelä, A., van den Broek, D., and Gregow, H.: Damaging thunderstorms in Finland in June 2021, Weather, 80, 111–119, https://doi.org/10.1002/wea.7602, 2025.

Weisman, M. L. and Klemp, J. B.: The dependence of numerically simulated convective storms on vertical wind shear and buoyancy, Mon. Weather Rev., 110, 504–520, https://doi.org/10.1175/1520-0493(1982)110<0504:TDONSC>2.0.CO;2, 1982.

Wennerdahl, E.: Change in Thunderstorm Activity in a Projected Warmer Future Climate: A Study over Europe, Dissertation, urn:nbn:se:uu:diva-337148, 2017.

Westermayer, A., Groenemeijer, P., Pistotnik, G., Sausen, R., and Faust, E.: Identification of favorable environments for thunderstorms in reanalysis data, Meteorologische Zeitschrift, 26, 59–70, https://doi.org/10.1127/metz/2016/0754, 2017.

WMO: World Distribution of Thunderstorm Days, WMO-No. 21, p. 213, https://library.wmo.int/idurl/4/37382, 1956.

Xie, K., Li, L., Chen, H., Mayer, S., Dobler, A., Xu, C.-Y., and Göktürk, O. M.: Enhanced evaluation of hourly and daily extreme precipitation in Norway from convection-permitting models at regional and local scales, Hydrol. Earth Syst. Sci., 29, 2133–2152, https://doi.org/10.5194/hess-29-2133-2025, 2025.